From: SELF-ORGANIZING SYSTEMS
Edited by F. Eugene Yates
(Plenum Publishing Corporatioin, 1987

29

Dynamics
A Visual Introduction

Ralph H. Abraham and Christopher D. Shaw

ABSTRACT

A dynamical system is one whose state may be represented as a point in a space, where each point is assigned a vector specifying the evolution. The basic ideas of the mathematical theory of dynamical systems are presented here visually, with a minimum of discussion, using examples in low dimensions. The "AB portrait" is introduced as a record of attractors and basins. The basic dynamical bifurcations also are given, including examples of bifurcations with two controls. Extensions of dynamical concepts are proposed in order to allow modeling of hierarchical and complex systems. These extensions include serial and parallel coupling of dynamical systems in networks.

The references for the ideas in this chapter can be found in Chapter 30. —THE EDITOR

While working together on the illustrations for a book, we discovered that we could explain mathematical ideas visually, within an easy and pleasant working partnership. Our efforts to illustrate "dynamics and self-organization" expanded inevitably into the work presented here. We use an animation technique familiar from *Scientific American* to develop the main ideas of dynamical systems theory, while relying as little as possible upon verbal descriptions. This style of presentation is at least ten times more costly than the usual verbal one. But then, a picture is worth a thousand words.

The ideas included are a mixture of ones familiar from the recent literature of dynamics and new ones based upon personal reflection. The reader should keep in mind that this is a personal view, and that the field of dynamics now is undergoing rapid evolution.

RALPH H. ABRAHAM • Division of Natural Sciences, University of California, Santa Cruz, California 95064. **CHRISTOPHER D. SHAW** • Department of Mathematics, University of California, Santa Cruz, California 95064.

Whitehead's (1925) *Science and the Modern World* describes the early history of dynamics in two periods—Galileo to Newton and Newton to Einstein—of the origins of modern science. Two further periods extend into the 20th century—Poincaré to Thom and Thom to the present. The ideas of Poincaré, originator of geometric dynamics, depart radically from the earlier concepts of Galileo and Newton. It is ironic that he is not mentioned by Whitehead, because Poincaré's great follower, George D. Birkhoff, was Whitehead's colleague at Harvard and was carrying on the new approach at the very moment Whitehead was writing his history. After Birkhoff, dynamics was dormant in the West, while the followers of Lyapunov, a Russian contemporary of Poincaré, continued the development of geometric techniques and concepts. This line of study was revived in the United States by the topologist Solomon Lefshetz (1950). Since then the field of dynamics has experienced tremendous expansion.

We present the basic concepts of dynamics in four historical groups: Galilean, Newtonian, Poincaréan, and Thomian. From antiquity to Galileo, general physical concepts of kinematics were developed, especially *space, time, curve of motion in space, instantaneous velocity at a point on the curve*, and *final motion* or asymptotic destination of the curve—probably thought to be a *limit point.* From Newton to Poincaré, the mathematical expression of "local" concepts flowered: *Euclidean space-time domain, integral curve, vectorfield*, and *attractor* (taken to be a limit point, or a *limit cycle*).

From Poincaré to Thom, the global geometric perspective emerged; the state space (or mathematical domain) of the dynamical system expanded from an open region in a flat Euclidean space to a *manifold*, or smooth space of arbitrary geometric and topological type. The dynamical system came to be viewed globally also: analytically, as a "flow" (or group of motions of the space of states upon itself); and geometrically, through its *phase portrait.* More complicated limit sets, such as the ergodic two-dimensional *torus of irrational rotation*, became known and the revolutionary concepts of *structural stability, generic property, and bifurcation* emerged. These concepts will be described in more detail below.

Thom developed the idea of *stable bifurcation*, as well as an even more global "big picture" of infinite dimension in which the stable bifurcations became geometric objects, amenable to classification. In the same period a new class of attractors, the *chaotic attractors*, was discovered experimentally, and a veritable industry of applications began. A parallel development, based on the analysis of invariant measures, has taken place in Russia. (The ideas of the Russian school are not included in this survey, although they are quite important.)

Dynamics

Mathematical dynamical systems (hereafter simply "dynamical systems") consist of deterministic equations, including ordinary differential equations, partial differential equations of the evolution type, or finite difference equations. The equations may occur singly or in sets.

Since Poincaré, dynamical systems have been studied using topological and

geometric methods, and dynamical systems theory has diverged from the classical analysis of differential equations and operators. A main goal of the geometric, or "qualitative," theory has been to understand the "final motions," or asymptotic limit sets, of a dynamical system. Here we present the most important ideas of dynamics through examples in low dimensions. The main idea is the "AB portrait" of a dynamical system, which records those aspects of the dynamics that are most evident in the qualitative point of view, the attractors and basins.

We proceed by presenting and describing 84 figures. In Chapter 30 the concepts will be applied to the problem of describing self-organizing behaviors.

Basic Concepts

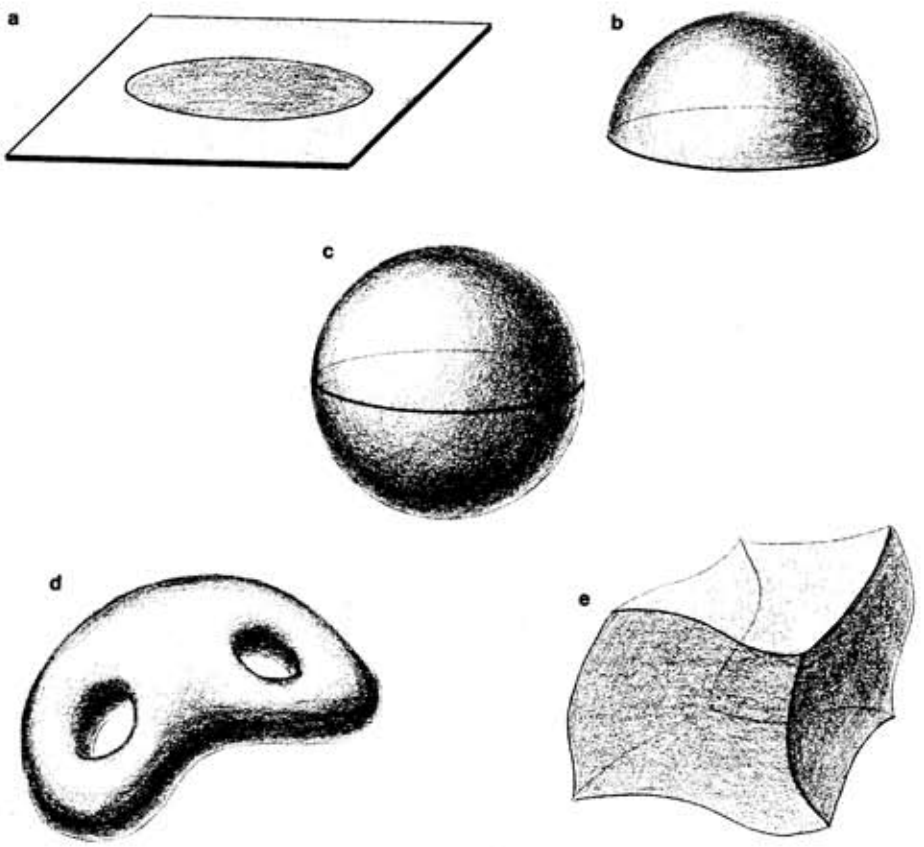

FIGURE 1. STATE SPACE. Many different spaces may be considered to be the domain of a dynamical system. Examples include: an open region in the plane (a); the upper hemisphere (b); the entire two-sphere (c); a closed surface with two holes (d); an open region of three-dimensional space (e); or a higher-dimensional surface. Each point of the state space corresponds to a "virtual state" of a system being modeled.

FIGURE 2. A DYNAMICAL SYSTEM on a state space consists of a vector assigned to each point. Each point in the state space is interpreted as a virtual state of the system modeled, as described above. Each of these based vectors is interpreted as a dynamical rule: the state must evolve with the speed and direction of the vector based there.

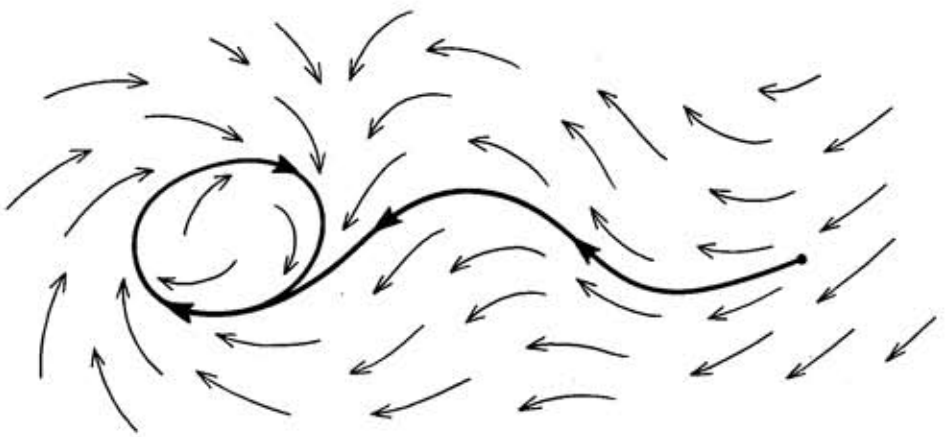

FIGURE 3. Starting at any point (a) in the state space, there is a uniquely determined curve (b) following the dynamical rules at each point it passes. The starting point is called the *initial state* (a); the curve (b) is its *trajectory*, and the asymptotic limit set of the curve (c) is the *limit set*. In these illustrations the curved arrows represent the *flow* of the dynamic, i.e., the simultaneous movement of all initial states along their trajectories.

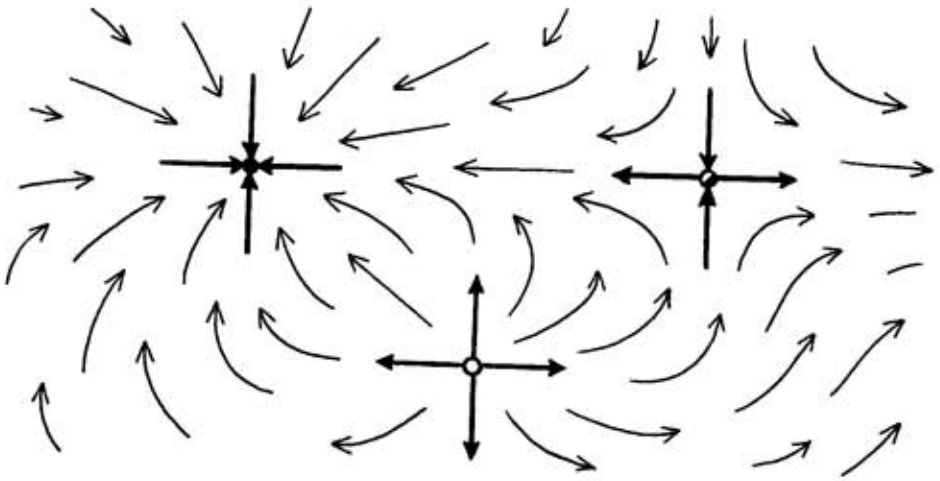

FIGURE 4. LIMIT POINTS IN TWO DIMENSIONS. The simplest limit set is a *limit point*. In two dimensions there are only three types of generic limit point: the point attractor (a); the point repellor (b); and the saddle point (c). In this context, the *inset* of a limit point refers to the set of all initial states which asymptotically approach the point in the future. The *outset* of the limit point comprises all initial states approaching the limit point as time (the parameter along the trajectory) goes backward. The saddle (c) has both inset and outset of one dimension. The attractive point (a) has a two-dimensional inset, called its *basin*. The repellor (b) has a two-dimensional outset.

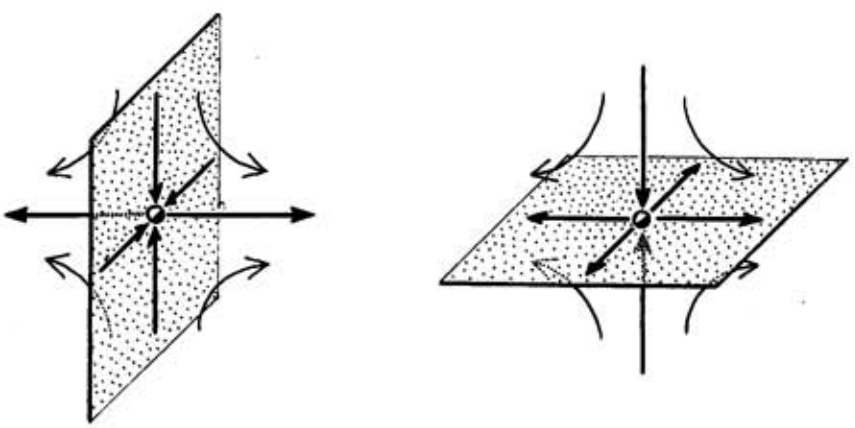

FIGURE 5. LIMIT POINTS IN THREE DIMENSIONS. Here attractors have three-dimensional insets, or basins, while repellors have three-dimensional outsets. There are two types of generic saddle: one has a two-dimensional inset (a); the other (b) has a one-dimensional inset.

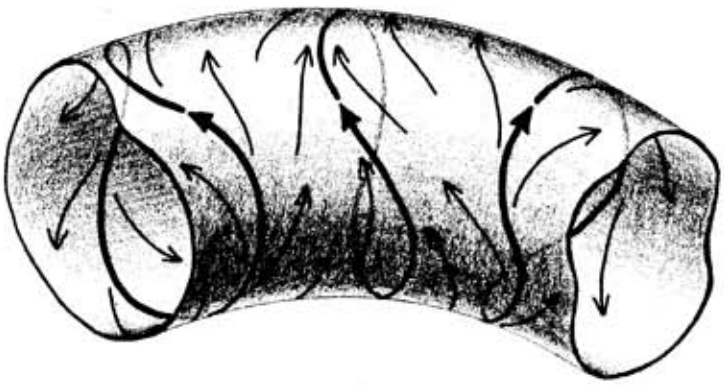

FIGURE 6. LIMIT CYCLES IN TWO DIMENSIONS. A circular limit set is called a *periodic limit set*, or a *limit cycle*. In two dimensions there are only two generic types, attracting (the *periodic attractor*) and repelling (the *periodic repellor*).

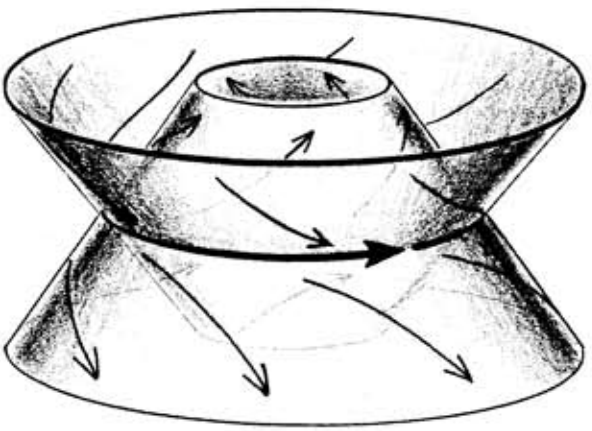

FIGURE 7. LIMIT CYCLES IN THREE DIMENSIONS. Here we have again the periodic attractor (three-dimensional inset) and the periodic repellor (three-dimensional outset), as well as a new type, the *limit cycle of saddle type*. Its inset is a two-dimensional cylinder, as is its outset. The two cylinders intersect in a circle, which is the limit cycle itself.

Basins and Separatrices

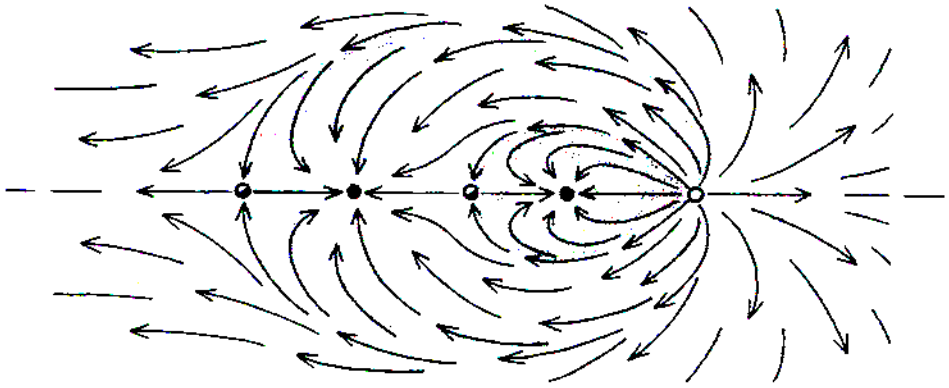

FIGURE 8. A *basin* is the inset of an attractor. A dynamical system usually has basins with one attractor in each. The state space is decomposed into a set of basins. The *probability of an attractor* is the relative area (or volume) of its basin. Here a dynamical system in two dimensions is shown, with three basins; two are shaded, and the third surrounds them.

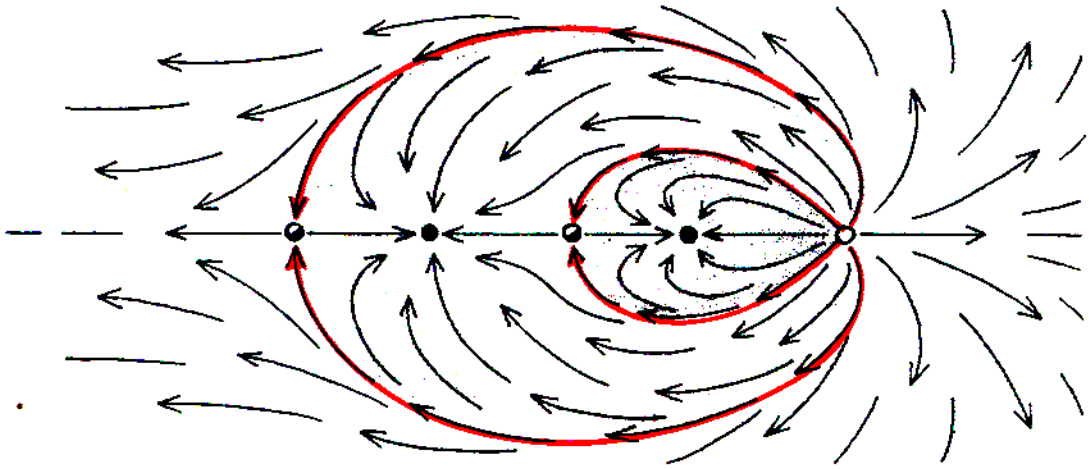

FIGURE 9. SEPARATRICES IN TWO DIMENSIONS. The *separatrices* are the boundaries of the basins. Usually we shall show these in red. By definition, separatrix points are not in basins. Thus, they belong to the insets of limit sets which are not attractors, the *exceptional limit sets*. Ideally, the probability of an initial point belonging to a separatrix should be zero. In this case, we may say that the separatrix is *thin*. The red separatrices here are the insets of saddle points. This picture of a state space, divided into basins by separatrices, with an attractor in each basin, is the *AB portrait* of the dynamical system.

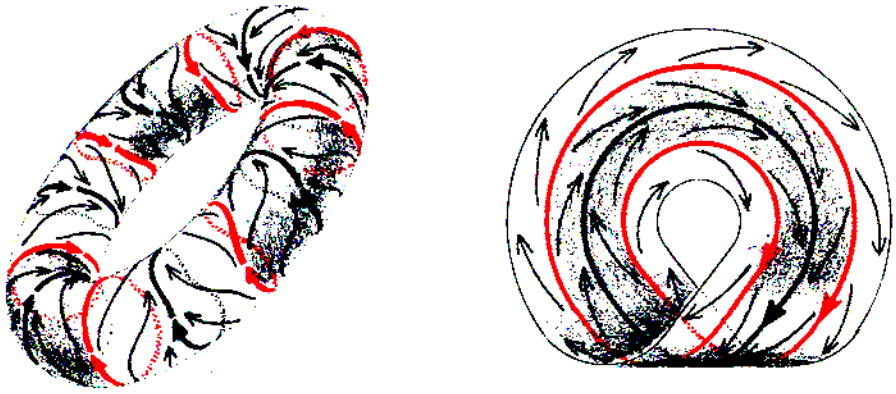

FIGURE 10. REPELLORS AS ACTUAL SEPARATRICES. In addition to the insets of exceptional (nonattracting) limit sets, the separatrix contains all the repellors of the dynamical system. These are the limit sets which would be the attractors if the arrow of time were reversed. Separatrices may be *actual* or *virtual*. Periodic repellors are shown here in dimension two. Because they actually divide the state space into distinct basins, they are actual separatrices. This occurs only in the two-dimensional case.

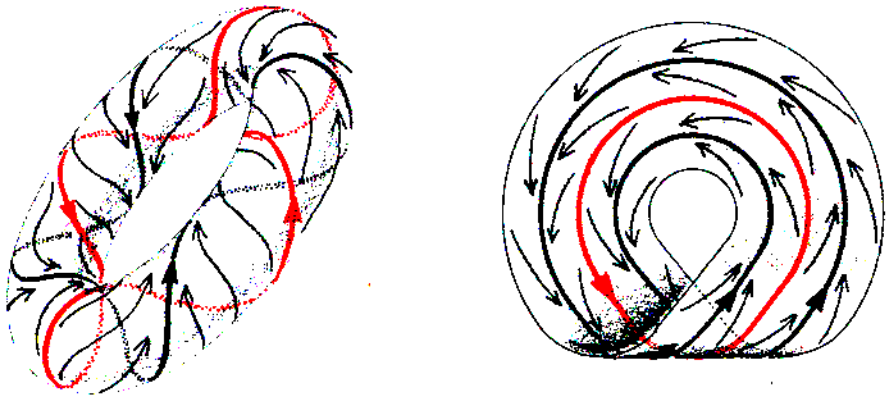

FIGURE 11. REPELLORS AS VIRTUAL SEPARATRICES. The periodic repellors in this figure do not divide the state space into distinct basins, because the state space with the red cycle removed has only one piece, the basin of the unique (black) periodic attractor. These periodic repellors therefore are virtual separatrices. Repelling limit points are also virtual separatrices.

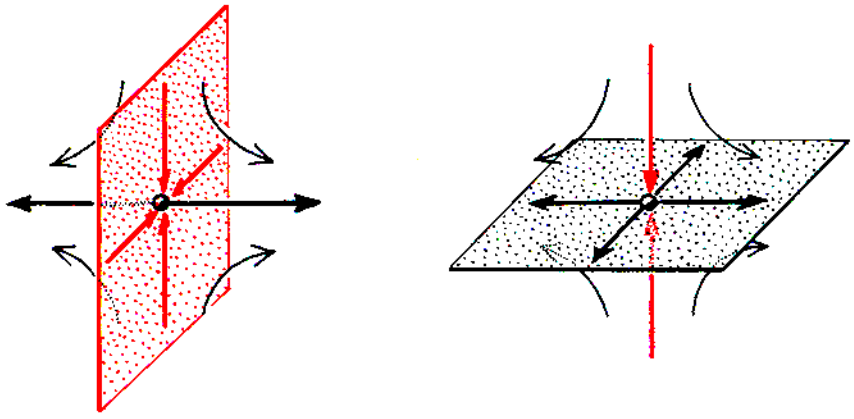

FIGURE 12. SEPARATRICES IN THREE DIMENSIONS. In two dimensions the separatrices are one-dimensional. In three dimensions they must be two-dimensional surfaces in order actually to separate the state space into disjoint regions. More generally, in "n-dimensions," they should have dimension "$n - 1$." Geometers call these "codimension one hypersurfaces."

This figure (similar to Figure 5) illustrates typical separatrices in three dimensions. The red surface, the inset of a saddle point, is called an actual separatrix because it actually separates the three-dimensional state space. The red curve, also the inset of a saddle point, is likewise a separatrix, but because it is not a codimension one hypersurface (it has codimension two) and cannot actually separate the space, it is called a virtual separatrix.

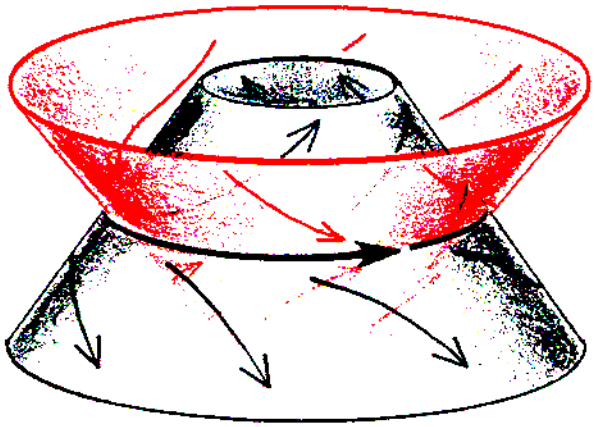

FIGURE 13. PERIODIC INSET SEPARATRICES. In three dimensions the periodic saddle (see Figure 7) is characterized by two cylindrical surfaces which pass through it, crossing through each other: the inset and the outset. The inset is a separatrix (as always) and therefore is shown in red. Furthermore, this inset has codimension one and is an actual separatrix.

Chaotic Attractors

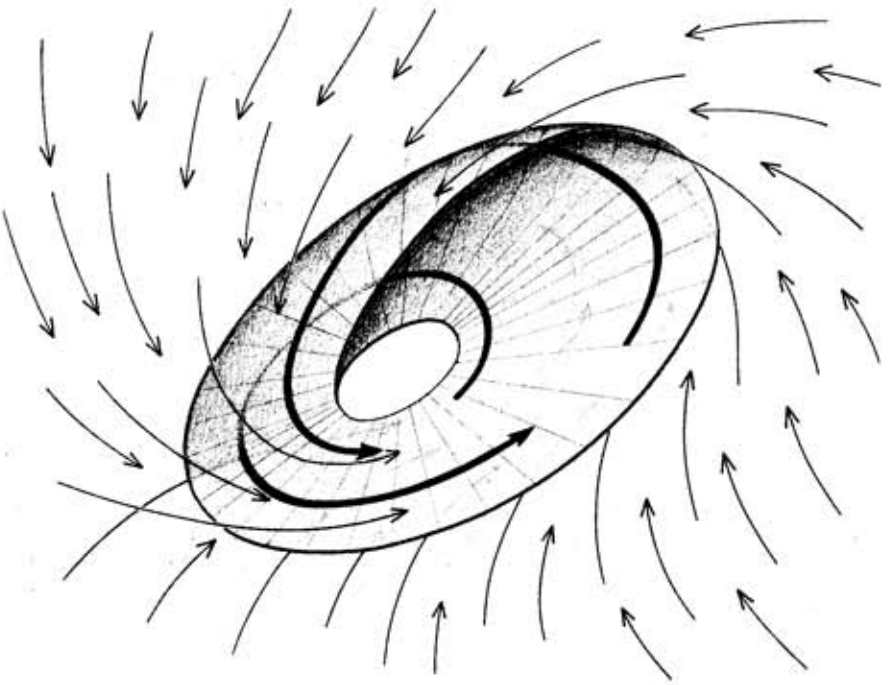

FIGURE 14. THE RÖSSLER. Beyond the point attractor (dimension zero) and the periodic attractor (dimension one) lives a little-known world of more complicated generic attractors. Most of these have been discovered by experimentalists; the one shown here was found by Rössler (an experimental dynamicist) with an analog computer. Like all of the attractors of dimensions greater than one, it is *chaotic* in the sense of power spectrum analysis; it emits broadband noise (Rössler, 1979). It is a *thick attractor*; although it looks two-dimensional, microscopic analysis reveals a *fractal* thickness. This attractor has "fractal dimension" 2+, i.e., a fraction more than two! The next six illustrations describe this "microscopic analysis."

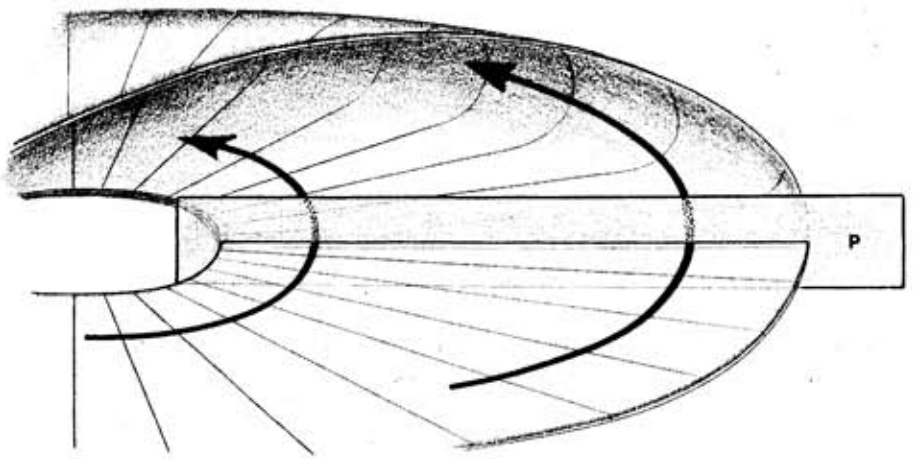

FIGURE 15. THE POINCARÉ SECTION. We cut through the attractor, in order to study its cross section, called the Poincaré section.

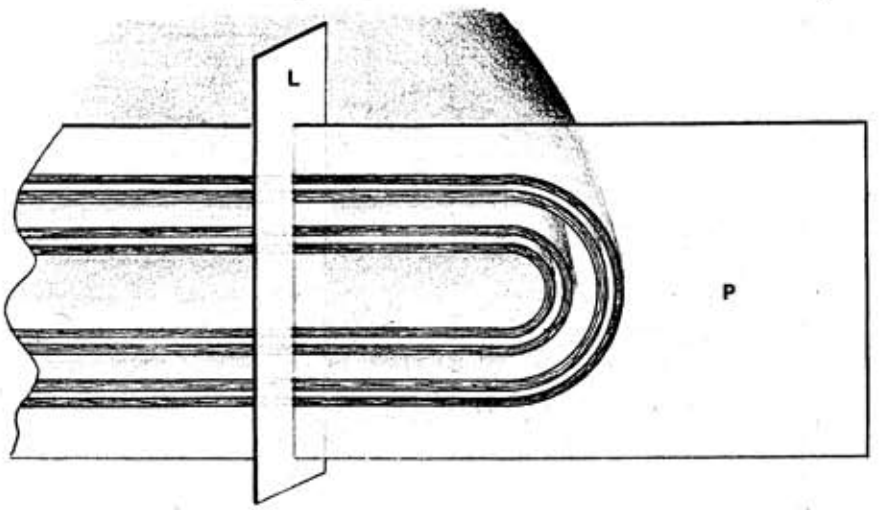

FIGURE 16. THE LORENZ SECTION. Enlarging the Poincaré section, we see that it consists of many curves compressed together. We cut through these curves with another cross section, as in Lorenz (1963).

FIGURE 17. THE LAYER SET. The second cut results in a line of dots, one for each curve of the Poincaré section, or, equivalently, one for each sheet of the Rössler attractor (Rössler, 1979). This result is a *Cantor set.*

FIGURE 18. CANTOR'S MIDDLE THIRDS CONSTRUCTION. The original Cantor set was constructed by removing the open middle third of a closed interval, followed by removal of the middle third of each of the two remaining intervals, *et cetera, ad infinitum*. The limit set contains no intervals. This Cantor set has fractal dimension 0.63 and linear measure zero.

FIGURE 19. THE MIDDLE FIFTHS CONSTRUCTION. Another Cantor set can be constructed by removing two fifths at each stage. This construction produces a Cantor set of fractal dimension 0.68 and zero linear measure. By removing smaller sectors at each stage, however, a limit set can by constructed which has positive linear measure, yet which contains no intervals. These are *thick sets*.

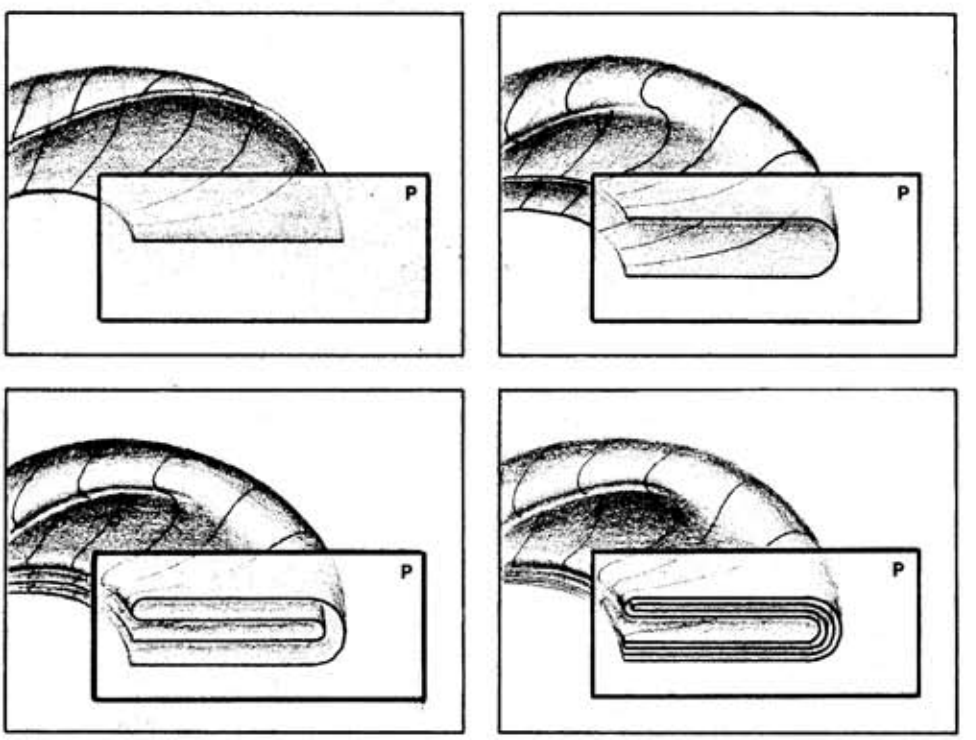

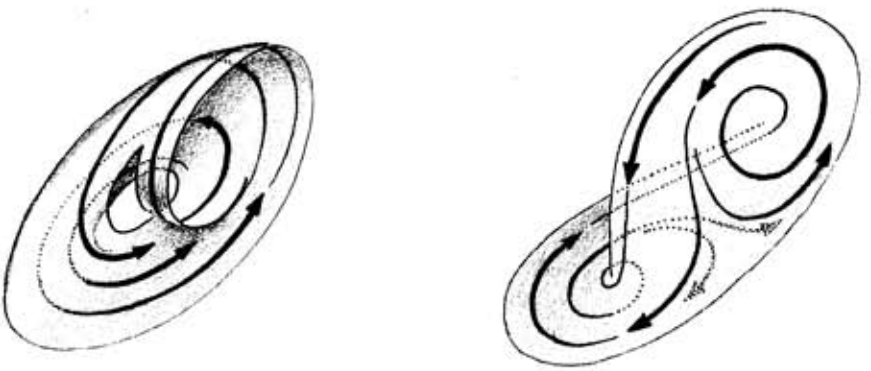

FIGURE 21. OTHER CHAOTIC ATTRACTORS. In addition to the Rössler attractor, many other attractors have been found by experiment. On the left is shown the *funnel*, also discovered by Rössler. Other attractors found by Rössler look amazingly like the seashells called tops, turbans, and sundials. On the right is the *Lorenz attractor*, the first to be found. This attractor was discovered in a digital simulation during Lorenz's study of atmospheric turbulence in 1961. These all seem to be *ergodic*, i.e., the averaging procedures of statistical physics apply to them.

←

FIGURE 20. THICKNESS OF THE ATTRACTOR. A Cantor set of two-dimensional sheets is a *Cantor 2-manifold* and has fractal dimension $2 + T$, where T is the fractal dimension of the Cantor set, measured across the layers. In this illustration we see why the Rössler attractor is a Cantor manifold. To the original Poincaré section across the Rössler attractor, we apply the *Poincaré section map*. Each point is carried once around the attractor, following the unique trajectory of the dynamical system, until it crosses through the Poincaré section again. Three iterations of this map are shown here. With each iteration, the section of the Rössler attractor is pulled out double-width, folded over, flattened, and reinserted into the section. The limit of this process is a Cantor manifold, and it covers the entire Poincaré section. We say the attractor is *fractal* if the fractal dimension is not an integer, and *thick* if the measure is nonzero (implying the same, integer dimension as the state space).

Separatrices also can have a Cantor structure; these are called *fractal* or *thick separatrices* by the same criteria of dimension and measure. In a thick separatrix, the probability of an arbitrary initial point belonging to the separatrix will be nonzero, but, one hopes, small. The limit sets of such initial points, which are not attractors, yet which have insets of positive volume, may be called *vague attractors*. In fact, some authors (e.g., Pugh and Shub, 1980) call even these "attractors."

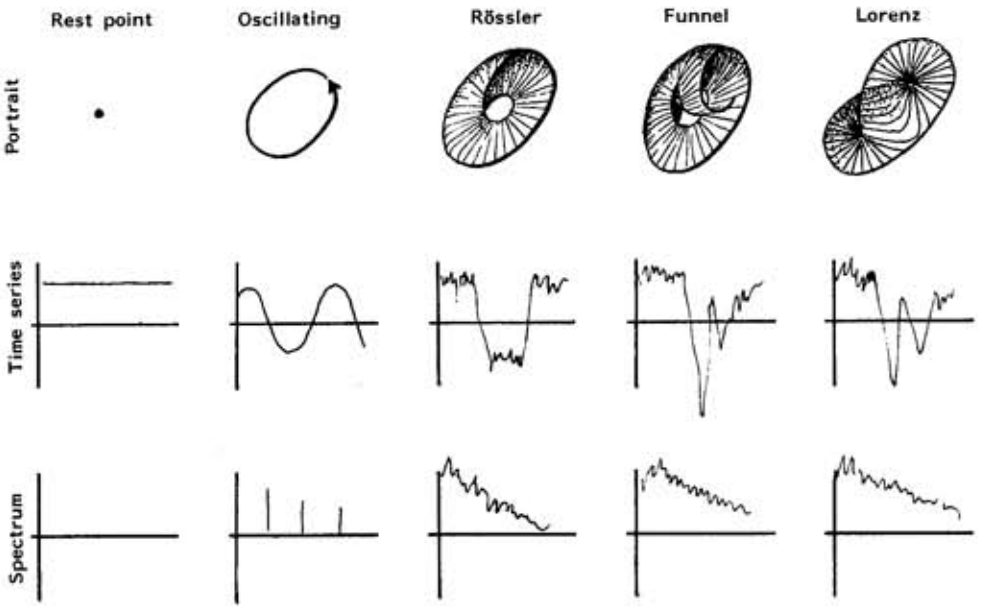

FIGURE 22. A LIST OF ATTRACTORS. Dynamicists would like to classify all generic attractors in some taxonomic scheme. While the end is not in sight, we have the beginning of a list. Here the list starts on the left, extending to the right beyond the five steps shown. Beneath each *attractor portrait* is its corresponding *time series* (or time record of a single coordinate of a trajectory along the attractor). Its corresponding *power spectrum* is shown beneath the time series. (The power spectrum is a plot of power versus frequency in the harmonic analysis of the time series.) Beneath the spectrum we could imagine a list of further attributes of the attractors across the top, adequate to distinguish them from one another.

Structural Stability

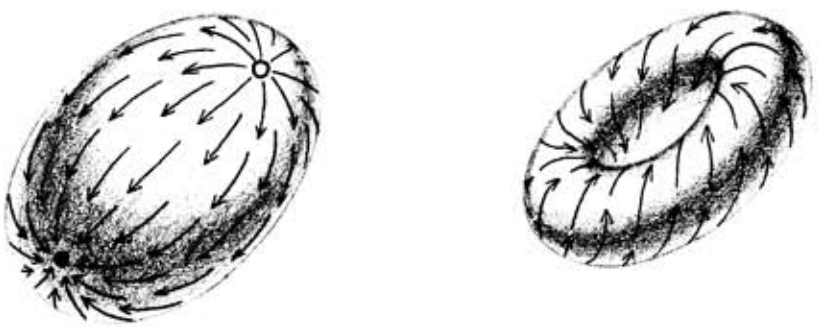

FIGURE 23. UNSTABLE ATTRACTORS. The system on the spheroid, at left, has a point attractor and a point repellor. It is *structurally stable*, in that any dynamical system obtained from it by a small perturbation will have essentially the same AB portrait. On the other hand, the system on the toroid, shown on the right, has no attractor other than the entire toroid. Its trajectories wind forever around it, like a solenoid. It is *structurally unstable*, because a small perturbation can change the AB portrait into a finite number of basins, each containing a closed orbit which winds several times around it (details are shown later).

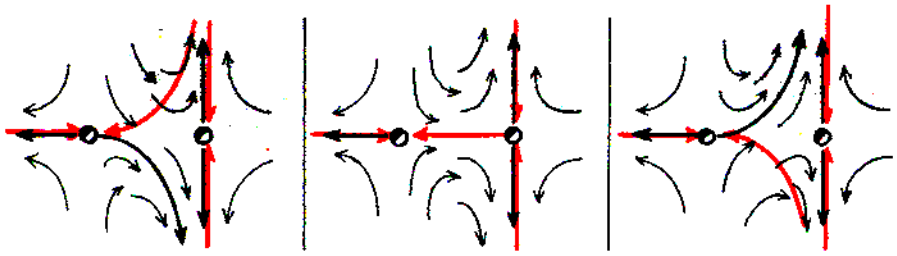

FIGURE 24. UNSTABLE BASINS. The dynamical system shown in the center has a *saddle connection*. A perturbation can produce the AB portrait on the left or the one on the right; these are essentially different (i.e., topologically nonconjugate) portraits. The attractors may be the same, but the basins are not. This sequence, read from left to right, is an example of *basin bifurcation*.

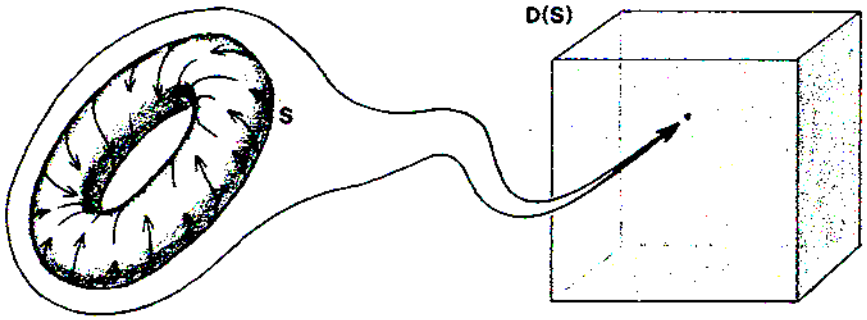

FIGURE 25. THE BIG PICTURE. An important overview of all dynamical systems on a given state space has been developed by Thom. Let S denote the given state space, e.g., a toroid, and $D(S)$ the set of all smooth dynamical systems on it. In this "big picture," a specific dynamical system corresponds to a single point.

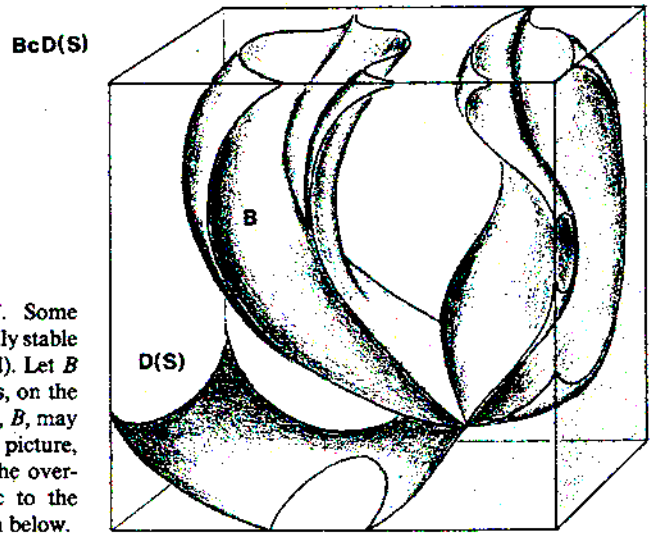

FIGURE 26. THE BAD SET. Some dynamical systems are structurally stable (good) while others are not (bad). Let B denote the set of all bad systems, on the given state space, S. The bad set, B, may be visualized within the big picture, $D(S)$. This account completes the overview of Thom, which is basic to the description of bifurcations given below.

Coupled Oscillators

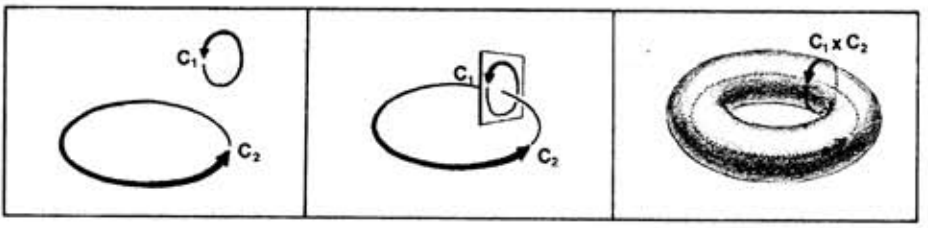

FIGURE 27. THE STATE SPACE FOR TWO OSCILLATORS. The state space for a single oscillator may be assumed to be a circle, C, of unit circumference. The dynamical system can be described as a constant velocity in the direction of the arrow, so that one full cycle has a period of V seconds and a frequency of $F = 1/V$ cycles per second. Now consider two such oscillators with state spaces denoted by C^1 and C^2 and frequencies F^1 and f^2. The state space for the combined system of the two oscillators is the torus, $C^1 \times C^2$.

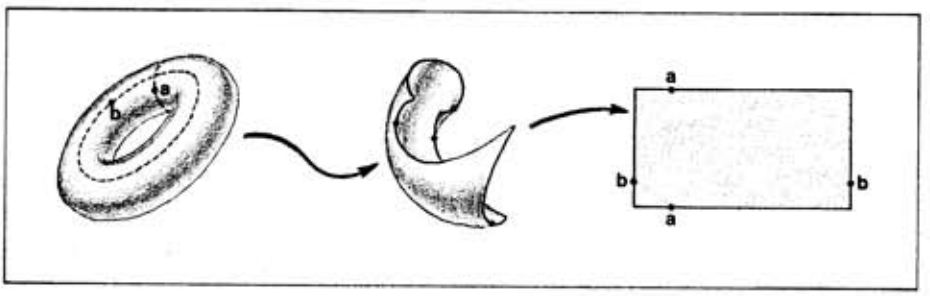

FIGURE 28. THE FLAT TORUS. For easier visualization we cut the torus along two circles, corresponding to the C^1 and C^2 "axes," and flatten it. To wrap it up again, identify (paste together) the two vertical edges, then the two horizontal circles. Thus, the two points labeled "a" represent the same point on the torus, as do the two points "b." Other than the boundary points, every point of the flat torus specifies a unique instantaneous state for each of the oscillators.

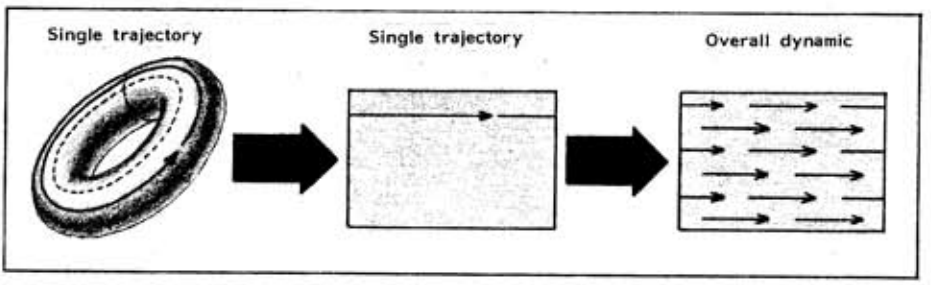

FIGURE 29. THE DYNAMIC FOR TWO OSCILLATORS. Suppose, for example, that the *second* oscillator is jammed or stuck ($F^2 = 0$). A trajectory on the real torus is then a horizontal circle, corresponding to a horizontal line on the flat torus, proceeding to the right with speed $V^1 = 1/F^1$.

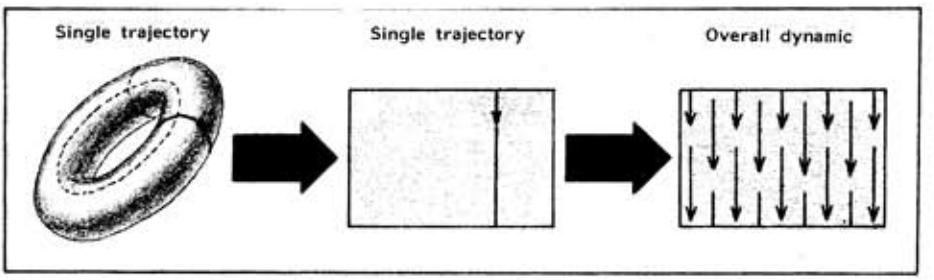

FIGURE 30. ANOTHER EXAMPLE. If the *first* oscillator is stuck, the dynamic is vertical, as shown here.

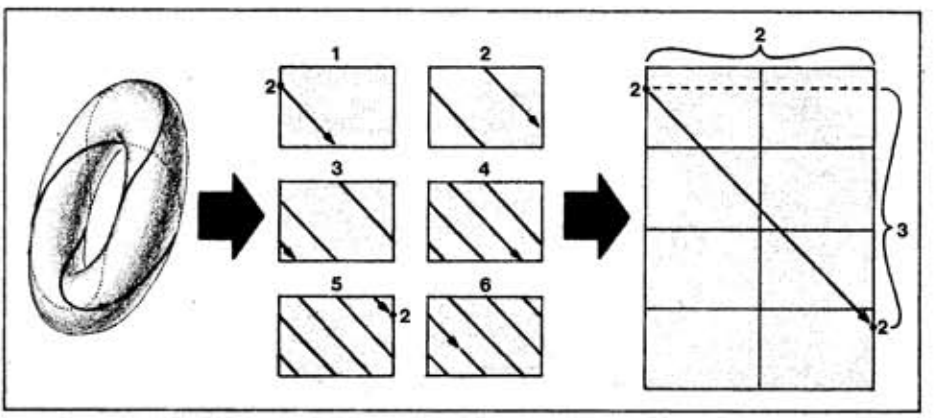

FIGURE 31. THE GENERAL UNCOUPLED CASE. When both oscillators are running, F^1 and $F^2 > 0$; the trajectories on the flat torus are still straight lines, with slope $V^2/V^1 = F^1/F^2$. For example, suppose this ratio of frequencies is $-3/2$. Thus, the first oscillator completes two cycles clockwise, while the second completes three cycles counterclockwise. The trajectories on the real torus are all closed cycles, or periodic trajectories, which wrap three times around the small waist (corresponding to C^2) and twice around the large waist. A full cycle of this compound oscillation is visualized best upon six or more copies of the flat torus, as shown here. This picture is modified easily to display the dynamic for coupled oscillators having any rational ratio of frequencies, or *rotation number*. The case of an irrational rotation number requires drawing a line of irrational slope across a doubly infinite array of flat tori, because the trajectories on the real torus never close.

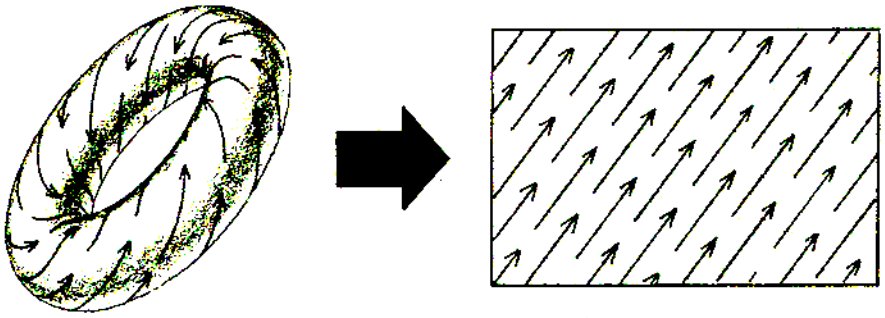

FIGURE 32. STRUCTURAL INSTABILITY. The uncoupled oscillators are structurally unstable, because a slight perturbation of the frequency of either (or both) will cause the rotation number to change through infinitely many rational and irrational values, each corresponding to an essentially different (topologically nonconjugate) portrait.

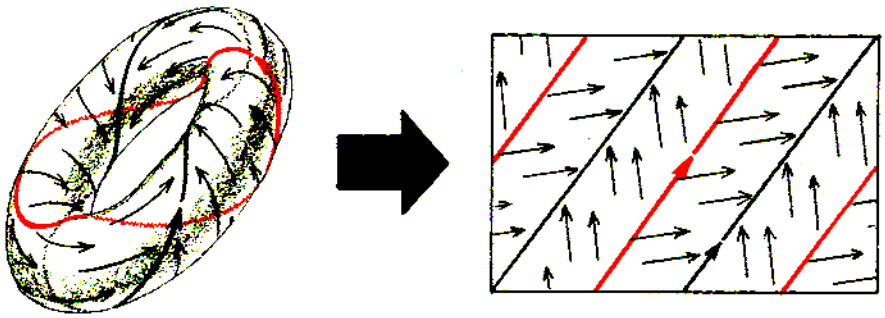

FIGURE 33. COUPLED OSCILLATORS. Coupling refers to a small (and unspecified) generic perturbation of the uncoupled dynamic previously described. The trajectories become wavy. According to the historically important *Peixoto theorem* (special to the two-dimensional case), the generic coupled dynamic must be structurally stable, having a finite number of basins,each containing a periodic attractor, and bounded by a periodic repellor. All of these limit cycles have the same period, determined by the rational rotation number of the dynamic. Because only these attractors can be found (as stable equilibria of the coupled oscillators), the oscillators are said to be *entrained*. The two oscillators, observed separately, are found to have frequencies in a rational ratio; therefore, an integral number of cycles of one oscillator takes the same time as another integral number of the other. Here we show a simple case, with only one basin and rotation number 1/2.

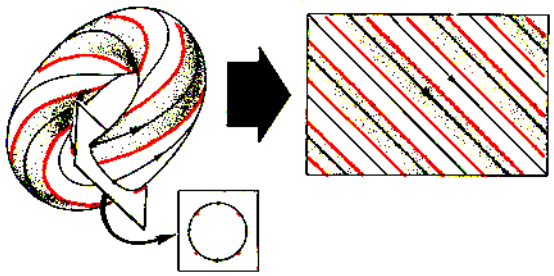

FIGURE 34. BRAIDS. The typical portrait for entrained (structurally stable or generically coupled) oscillators has many basins, braided together around the real torus. Their visualization is facilitated by cutting through the torus with a plane, obtaining a circular cross section, the Poincaré section. This circle is punctuated by alternating red points (where separatrices cross) and black points (corresponding to attractors). Here we show a 2-braid. There are two distinct basins, one of which is shaded. Each has rotation number -3/2, as in Figure 31.

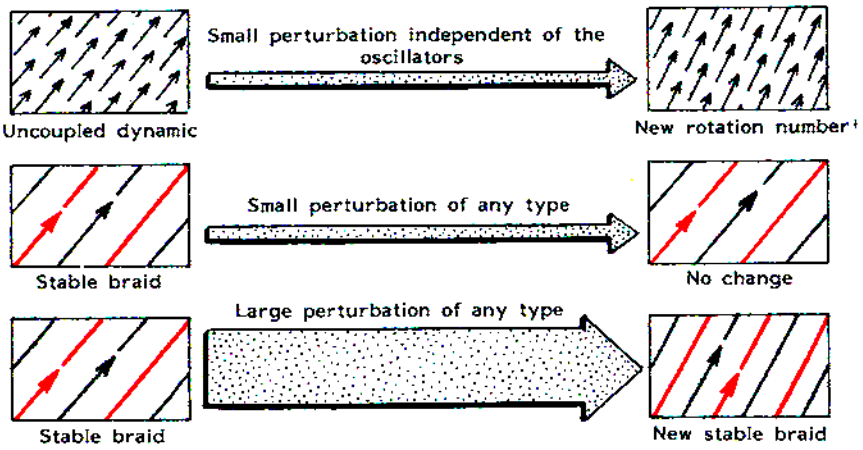

FIGURE 35. ENTRAINMENT IS STABLE. While uncoupled oscillators are structurally unstable (Figure 32), two generically coupled oscillators are stable, according to Peixoto's theorem. Even so, a large perturbation can change one stable braid into another.

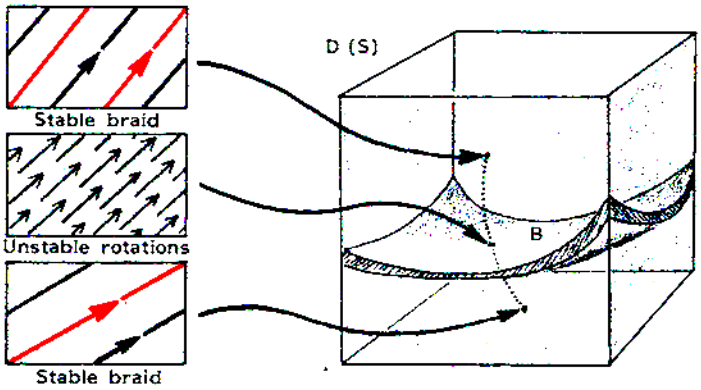

FIGURE 36. THE BIG PICTURE OF ENTRAINMENT. Because each dynamic on the torus is represented by a single point in the big picture, the transition of one stable braid into another by perturbation can be represented by a dotted line. An intermediate dynamic with an irrational rotation number must belong to the bad set.

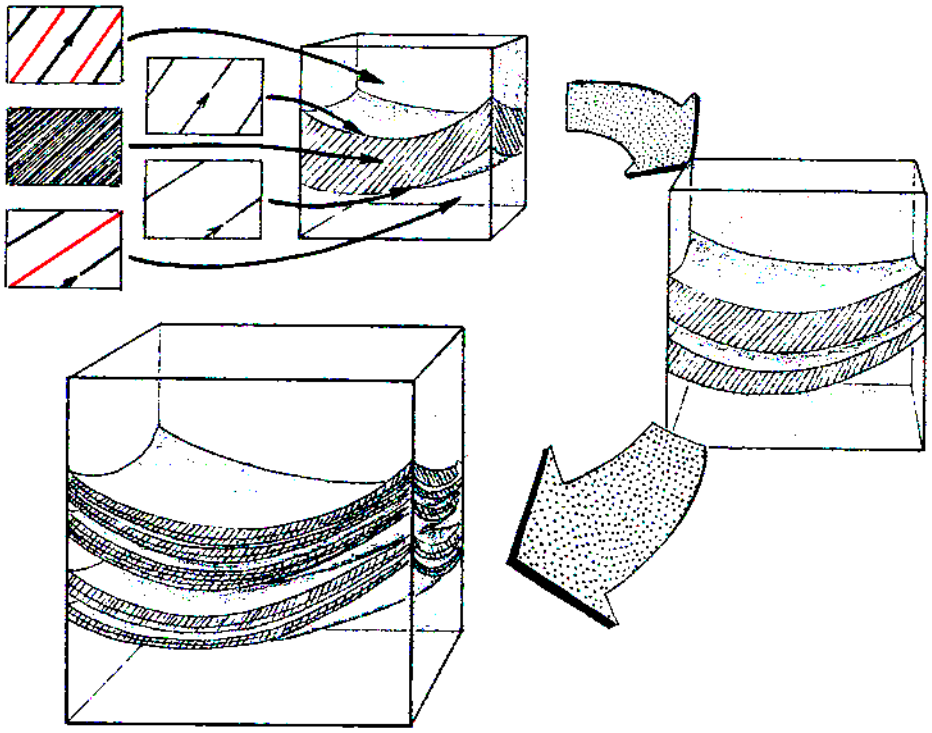

FIGURE 37. THE MICROSTRUCTURE OF THE BAD SET. Suppose the transition of one stable braid into another is made continuously. The rotation number of the initial braid then changes continuously into the rotation number of the final braid. Between these two rational numbers are infinitely many irrationals. The bad set, therefore, must have an infinite set of layers, pressed very closely together. It has been shown that this bad set is a thick Cantor manifold (see Figure 20) in some general sense.

Bifurcations

Dynamical bifurcation refers to the continuous deformation of one dynamical system into another inequivalent one, through structural instability. One must be careful not to confuse Dynamical Bifurcation theory (created by Poincaré in 1885), which is the subject of this survey, with the somewhat similar subjects of Elementary Catastrophe theory or Classical Bifurcation theory. These are compared in Chapter 30.

The most important applications of dynamical systems theory demand the inclusion of controls in the model. The full accommodation of this demand into dynamical systems theory first occurs in Thom's (1972) *Structural Stability and Morphogenesis*. Here we present a visual account of the basic notions of dynamical bifurcation, along with a selection of the simplest bifurcations.

Catastrophic Bifurcations

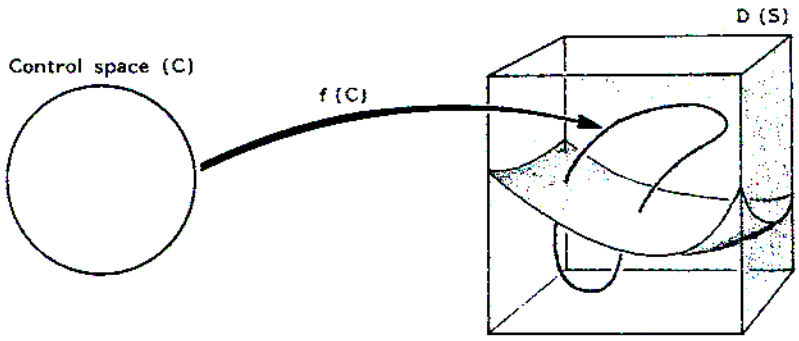

FIGURE 38. DYNAMICS WITH ONE CONTROL. The states of the controller are modeled by an auxiliary space, the control space, C. In this section, we consider only the case of a single control; the dimension of C is one. Here, C is shown as a circle. An auxiliary function, f, maps the control space into the big picture. For each "setting of the control knob," represented by a point c of C, there is, therefore, a corresponding dynamical system $f(c)$ on the given state space, S. As c is moved along C, $f(c)$ moves smoothly within the big picture, and the dynamical system on S changes smoothly as well.

As long as $f(c)$ does not cross the bad set, B, the AB portrait of the dynamic on S does not change in any essential way. After traversing B, however, the portrait is essentially different (i.e., it is topologically nonconjugate). These transformations are known as *bifurcations*. In the best cases, the image of the control space within the big picture, $f(C)$, crosses cleanly through the bad set, B. These cases, called *generic bifurcations*, are the main target of Thom's program. The generic bifurcations with one control are also called *generic arcs*.

In the applications of dynamics with controls, the modeling function—or *morphogenetic field*, as Thom called it—cannot be specified exactly. Thus, *stable bifurcations*, which are insensitive to perturbations of the modeling function, f, are the events most important to know.

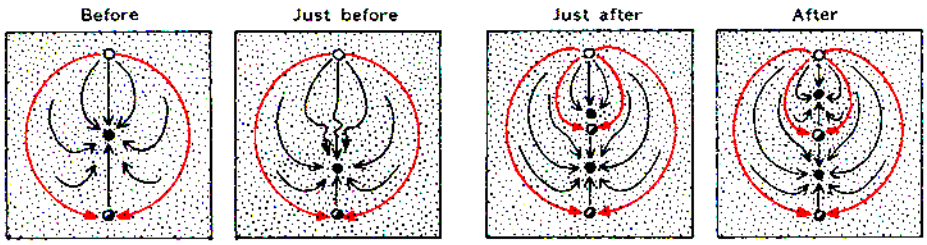

FIGURE 39. STATIC CREATION. Here are four frames from a "movie" of the simplest stable arc, from left to right. At first there is a single point attractor in the center of its basin. Next, the trajectories approaching it from above are pinched together, like a pigtail. This change is caused by a turn of the "knob" and, as yet, there has been no bifurcation. In the third frame there are two point attractors, each in its own basin. The new one is just above a new saddle point, which was created at the same moment, or control setting, called the *bifurcation point* in the control space. In the last frame, the new attractor has receded further from its companion saddle, and, thus, also from the separatrix bounding its basin. This event, sometimes called the *saddle-node bifurcation*, is similar to the *fold catastrophe* of Elementary Catastrophe theory.

When this "movie" is shown in reverse sequence, the upper attractor drifts toward the edge of its basin. At the bifurcation point, it collides with a saddle in the separatrix. The attractor and separatrix simultaneously vaporize, or disappear "into the blue." This event is called *static annihilation*.

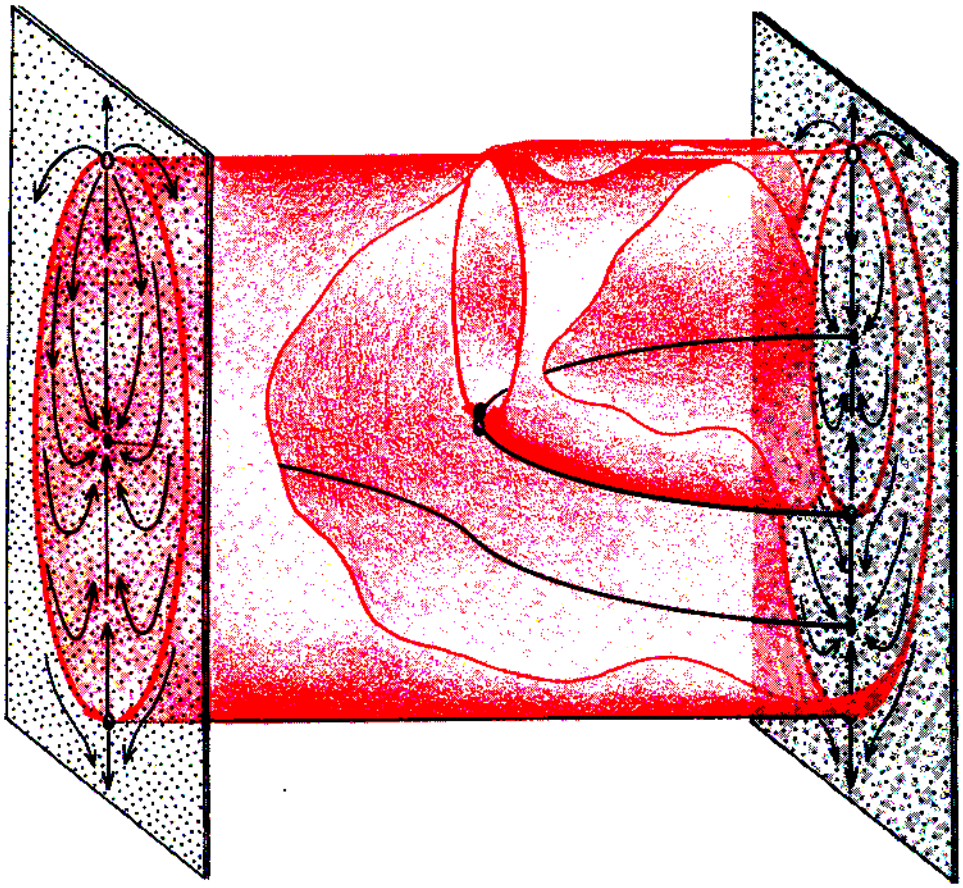

FIGURE 42. BIFURCATION DIAGRAM OF STATIC CREATION. Here is the filled-in portrait for the static creation bifurcation of Figure 39. This is a *catastrophic bifurcation* in the sense that the track of the upper attractor appears "out of the blue," i.e., far from any other attractor.

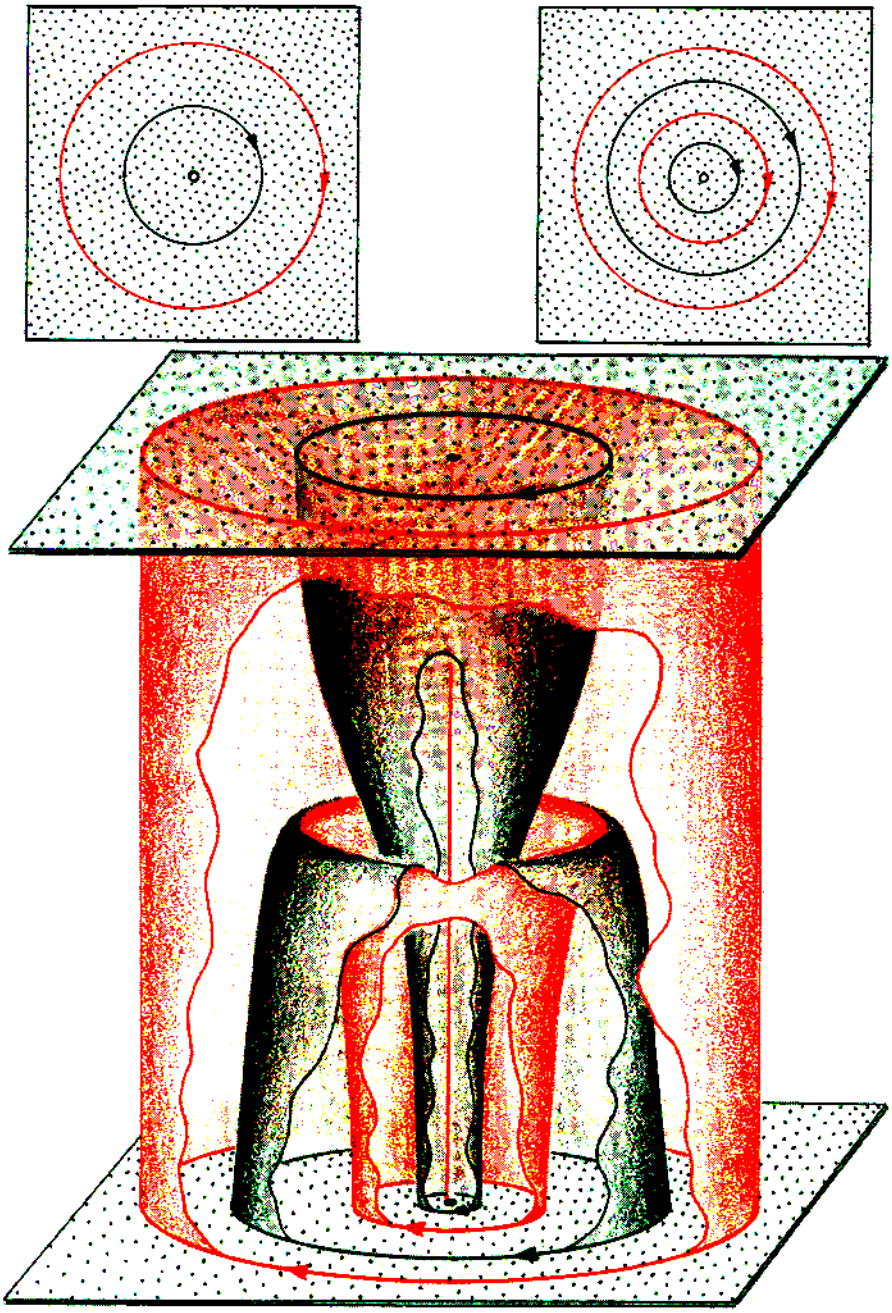

FIGURE 43. CREATION OF AN OSCILLATION. This is the second of the simple bifurcations. In this event a periodic attractor appears catastrophically. Before the creation event, a periodic attractor (black) is shown in a basin bounded by a periodic repellor (actual separatrix, red) and a point repellor (virtual separatrix, red). Without change in these three elements, the AB portrait after the event has two new elements, a periodic attractor and a periodic repellor. The bifurcation diagram shows how these two elements were created simultaneously, as the control moved past the bifurcation point in the control space. The new periodic repellor is the separatrix of the new basin of attraction. Were this movie to be viewed in reverse, we would see the inner attractor growing, until it approached the boundary of its basin and touched it, causing both elements to vaporize at once. This is a typical annihilation catastrophe and is also known as *hard self-excitation.*

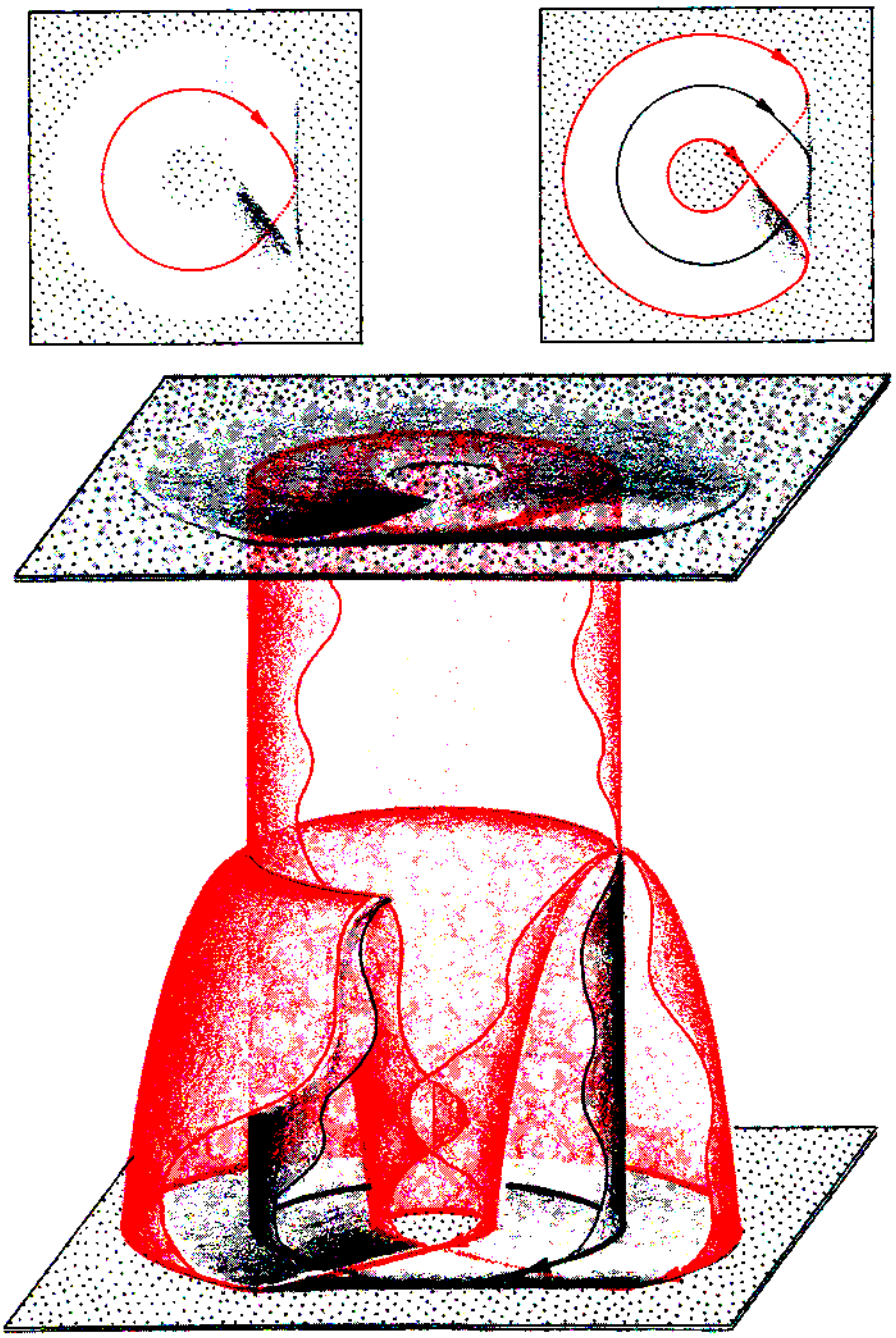

FIGURE 44. CREATION OF AN OSCILLATION. This is another type of catastrophic creation of an oscillation. The state space, S, is a Möbius band. Before the creation event, a periodic repellor circles the Möbius band. Empirically invisible, it is a virtual separatrix; hence, it is shown red here. After the event it has become an attractor, and thus is shown in black. The new separatrix bounding the basin of this attractor circuits the Möbius band twice before closing. The bifurcation diagram reveals the details of the transformation process. At the instant the red cycle turns black, the new separatrix branches off, rather like a paraboloid of revolution. We could view this bifurcation as an explosion, in which a virtual separatrix thickens, creating a new basin. A new attractor has appeared suddenly.

Hysteresis

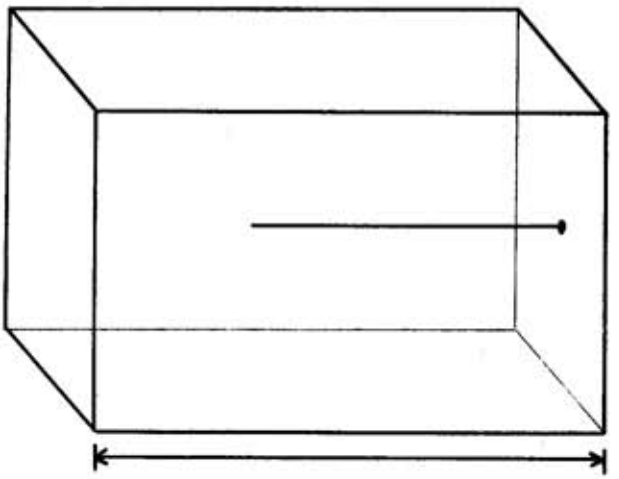

FIGURE 45. CATASTROPHIC BIFURCATION involves the sudden creation of a new basin and attractor, as in the three examples of the preceding section.

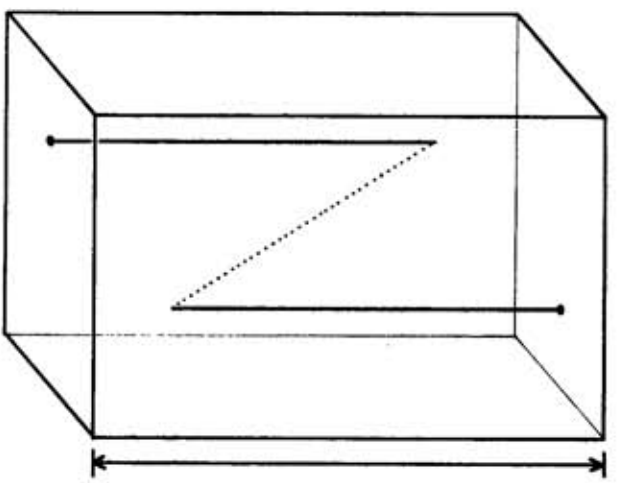

FIGURE 46. HYSTERESIS occurs in a bifurcation diagram containing at least two catastrophic bifurcations, back to back. In this example a static creation is followed by a static annihilation, as in the *fold catastrophe* of Elementary Catastrophe theory. We shall refer to this configuration as a *hysterical kink.*

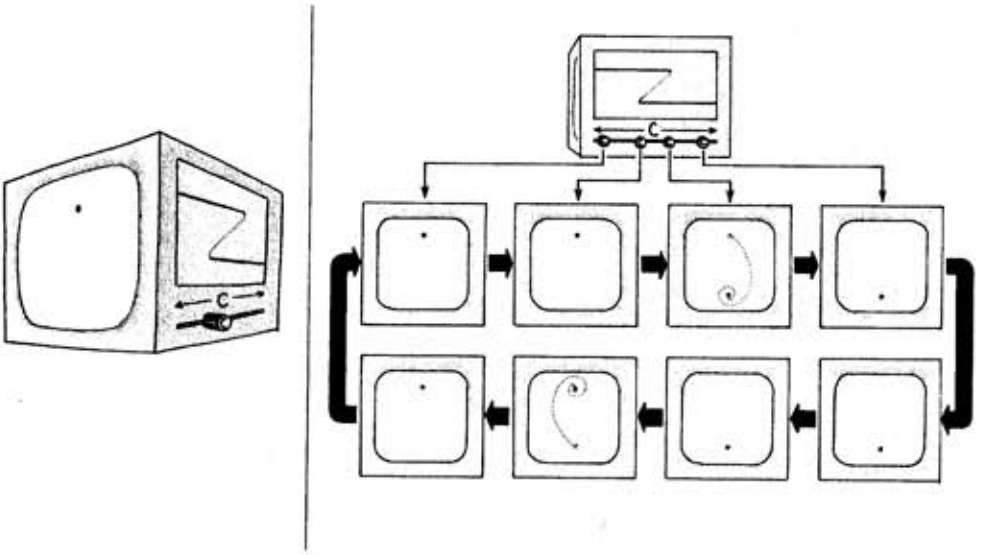

FIGURE 47. A HYSTERESIS LOOP is shown here, in a mechanical representation, realizing the preceding bifurcation diagram. Beginning with the control full left, the knob is moved to the right. The sequence of observations in the top row results. Initially the system is caught in the upper attractor. After the knob passes the first bifurcation point in the control interval, a second attractor exists. The machine, however, does not reveal it; there is no change of behavior. After the knob passes the second bifurcation point, the upper attractor vanishes (after colliding with its separatrix, which slides along the dotted track), and the machine finds itself in the far reaches of the basin of the lower attractor. The dynamic asserts itself, the current state rushes toward its new attractor far below, the transient dies away, and the machine settles down to its new equilibrium. The knob is full right.

Next the knob is pushed slowly back to the left. After a similar sequence, the screen shows that the machine again has settled down in the original attractor, near the top. The transition upward occurs near the left bifurcation point, however, after passing the control point of the downward transition. This is the classical hysteresis loop behavior. In the context of Dynamical Bifurcation theory it has many more complicated forms.

Subtle Bifurcations

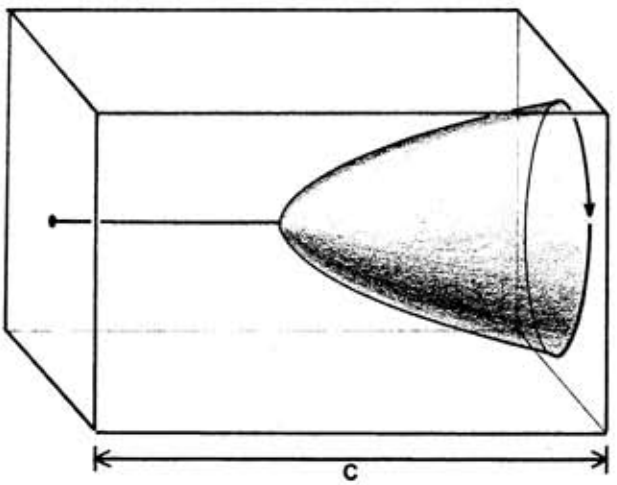

FIGURE 48. SUBTLE BIFURCATIONS differ from catastrophic ones in that nothing new appears suddenly out of the blue. Instead, an existing attractor changes gently into another type of attractor. In the bifurcation diagram shown here (and discussed below) a point attractor changes into a periodic attractor. The change is noticed only after the amplitude of the oscillation has grown large enough to be observed.

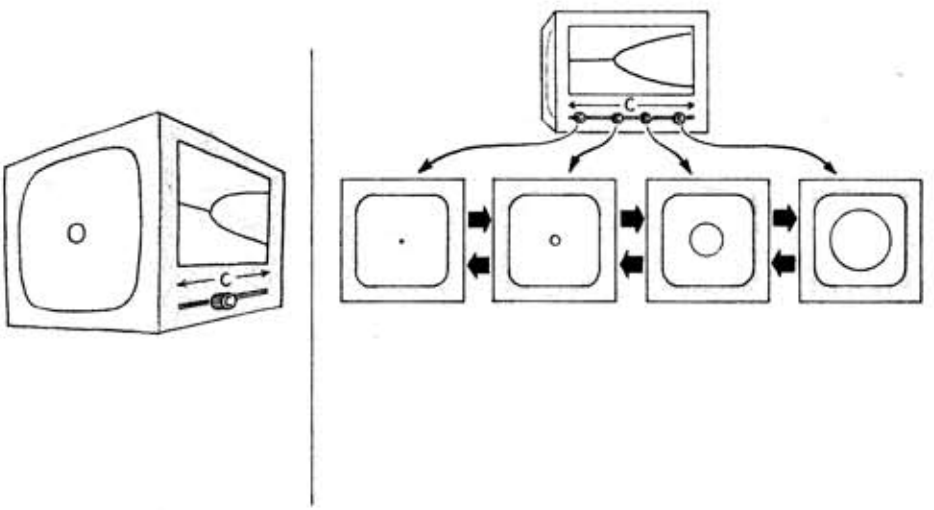

FIGURE 49. MACHINE REPRESENTATION of a subtle bifurcation shows that the attractor under observation, a point attractor, changes into an oscillation as the control is moved to the right. The amplitude increases as the control is moved more to the right. As the control is returned to the left, the same sequence is observed in reverse. The amplitude of the oscillation decreases, and the circle shrinks to a point. The death of the oscillator occurs at the same bifurcation point at which it first appeared. There is *no hysteresis* with subtle bifurcations.

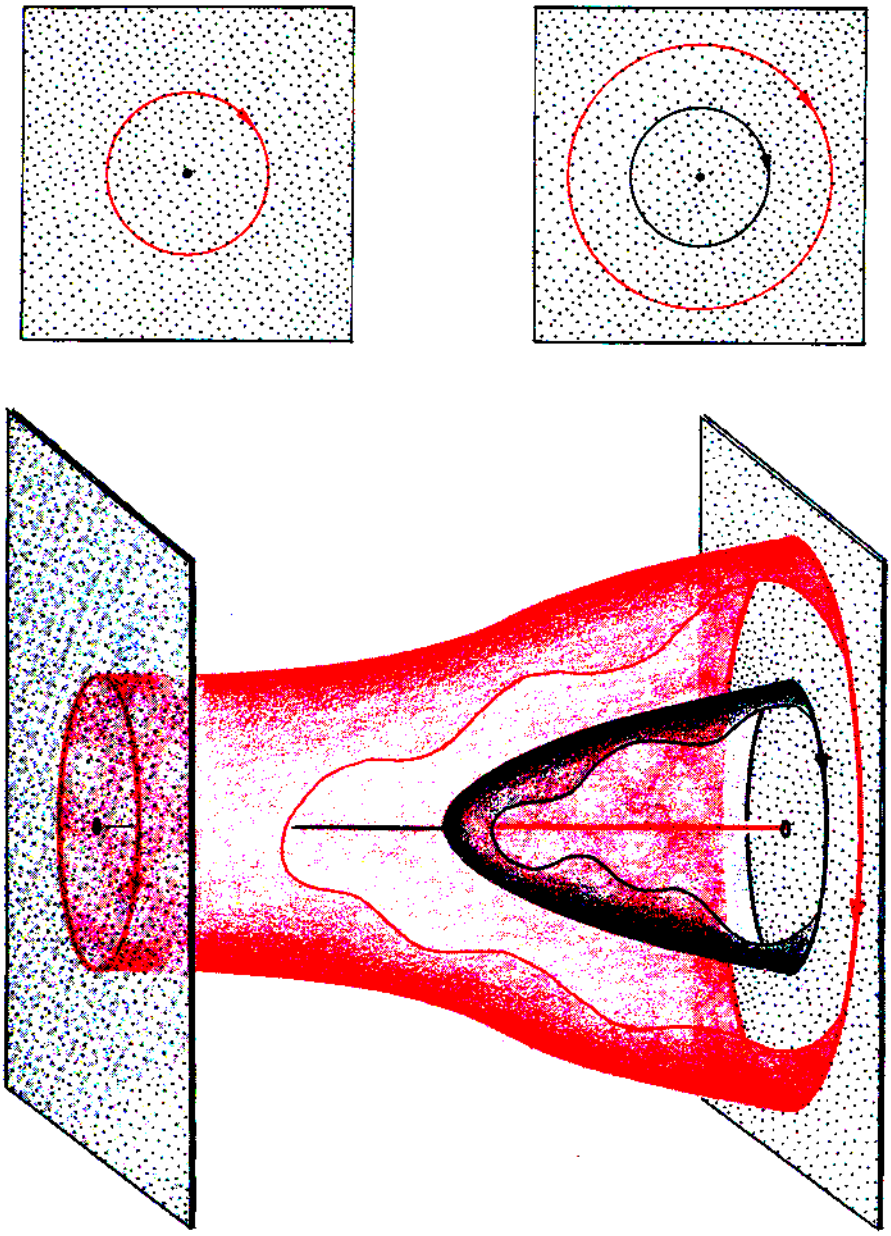

FIGURE 50. EXCITATION. This event, also known as the *Poincaré-Andronov-Hopf bifurcation*, is an outstanding example of subtle bifurcation. Without actual change of basin, the point attractor turns into a periodic attractor. An oscillation has been born. Again, the bifurcation diagram shows how the amplitude of the new oscillation grows parabolically as the control moves to the right. This event may provide a dynamical model for the morphogenesis of the flat rings of Saturn.

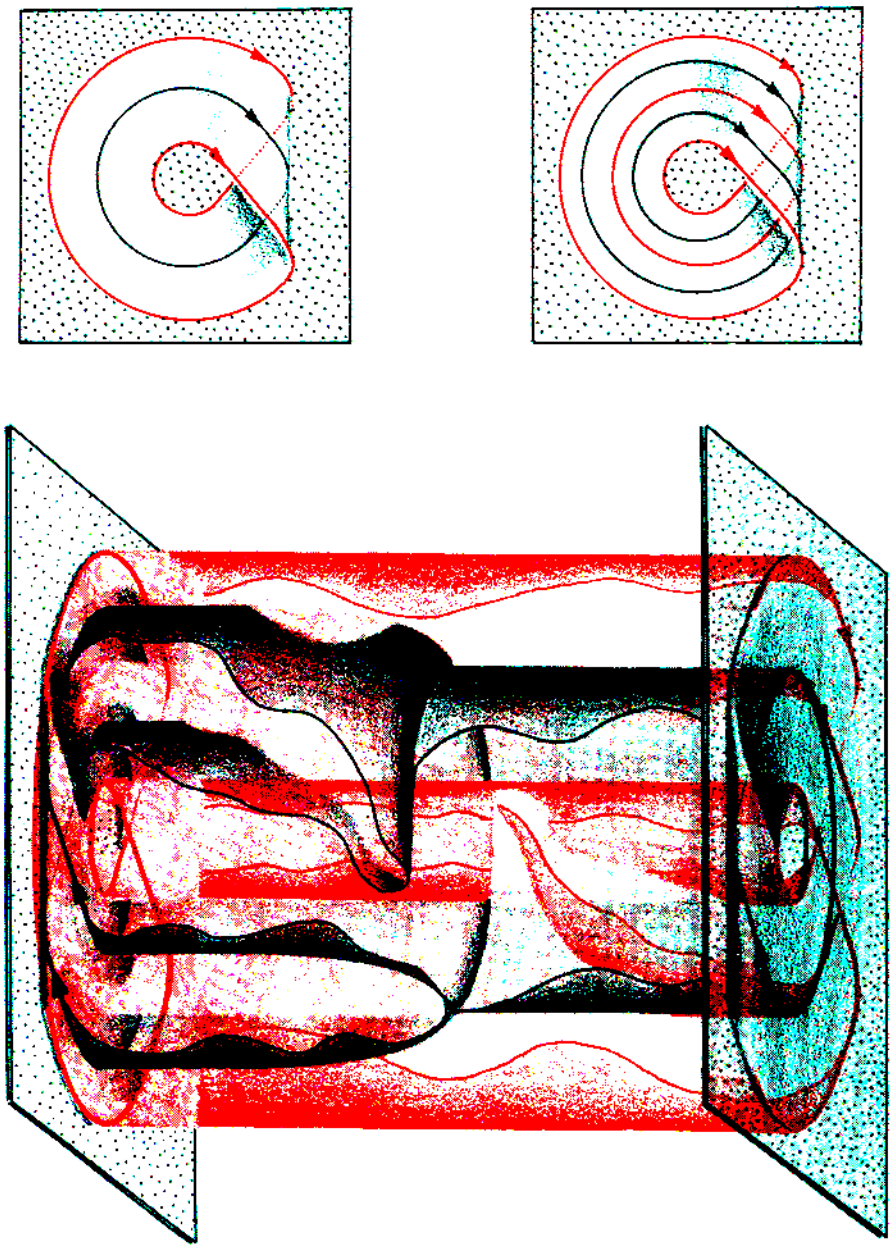

FIGURE 51. THE OCTAVE JUMP. Before bifurcation a periodic attractor (black) circles the Möbius band in a basin bounded by an actual separatrix (periodic repellor, red) which circuits twice before closing. After the event the original attractor becomes a virtual separatrix (periodic repellor, red) in the basin of a new periodic attractor (black). The outer boundary of this basin is the same separatrix as previously. The new attractor has twice the period and half the frequency of the original one, and is appropriately named. The bifurcation diagram shows the whole sequence of this event, which is a subtle bifurcation in the sense that the jump down an octave becomes noticeable gradually, as in a slow yodel. No attractor track has appeared "out of the blue."

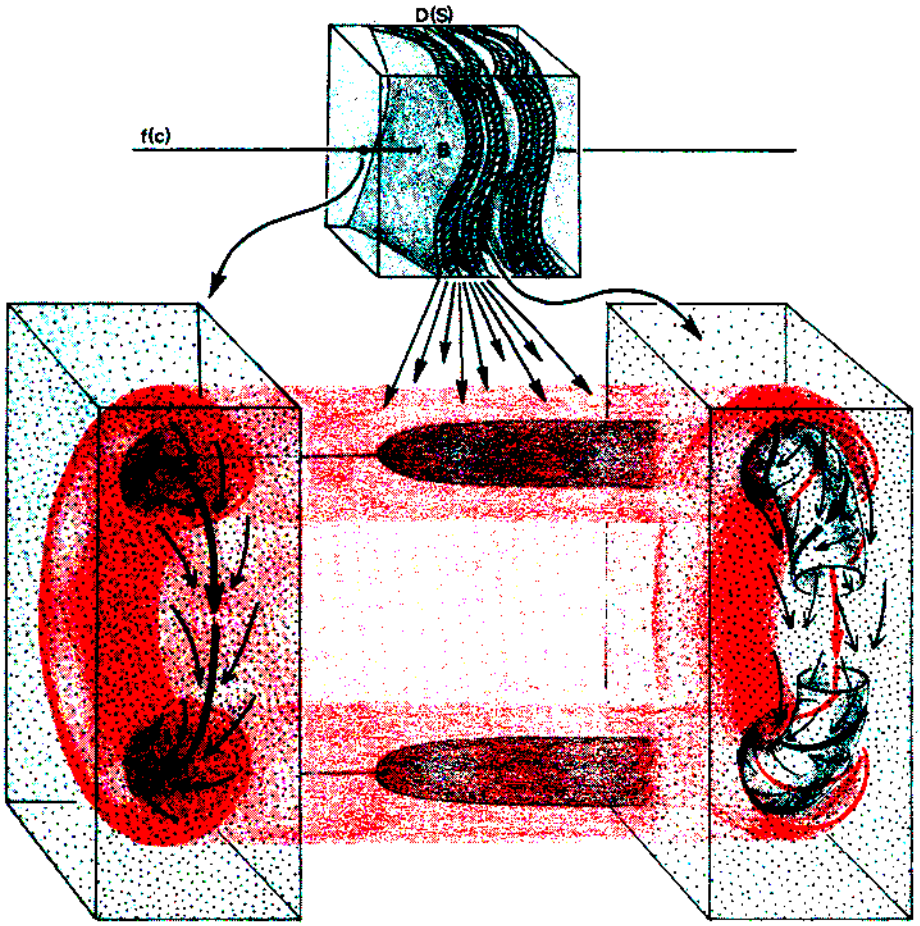

FIGURE 52. EXCITATION OF A TORUS. This is a subtle bifurcation, closely related to the excitation of an oscillation (Poincaré–Andronov–Hopf bifurcation, Figure 50), shown previously. Coarsely observed, it resembles a single event. Before the event there is a single periodic attractor in a three-dimensional basin. For simplicity the boundary of its basin is shown as a torus, although this is not frequent. After the subtle bifurcation, the periodic orbit is changed to a repellor (red circle) within a thin torus (black) on which a braid (see Figure 34) is shown. The torus is *attracting, yet not an attractor.* The new attractors, after the event, are the periodic attractors within the braid on the torus. These fluctuate, however, among many different (and topologically inequivalent) types of braids immediately after the creation of the torus, as described in the discussion of the coupled oscillator (see Figure 37). This event thus includes a Cantor set of bifurcation points in the control space, illustrated here by a small piece of the big picture. We call this a *thick bifurcation* because the set B^f of bifurcation points in the control space, C, is a thick Cantor set. The probability of observing a nonstructurally stable attractor (in this case it would be an attracting torus—a "miracle" from the point of view of structural stability dogma) is the measure of the bifurcation set, B^f. Because this is a positive number, we have here a model for the expectation of "miracles." This multiple bifurcation event was discovered, bit by bit, in the work of Neimark (1959), Peixoto (1962), Sotomayor (1974), and Herman (1979), and may be called the *fluctuating braid bifurcation.* This event may provide a dynamical model for the morphogenesis of the braided rings of Saturn.

There are further excitations in which an attractive, two-dimensional torus becomes an attractive, three-dimensional torus, and so on, through higher modes of oscillation. The relaxation of the dynamics on these tori into structurally stable systems comprises the extension of the entrainment idea to coupled systems of several oscillators. The details are as yet unknown.

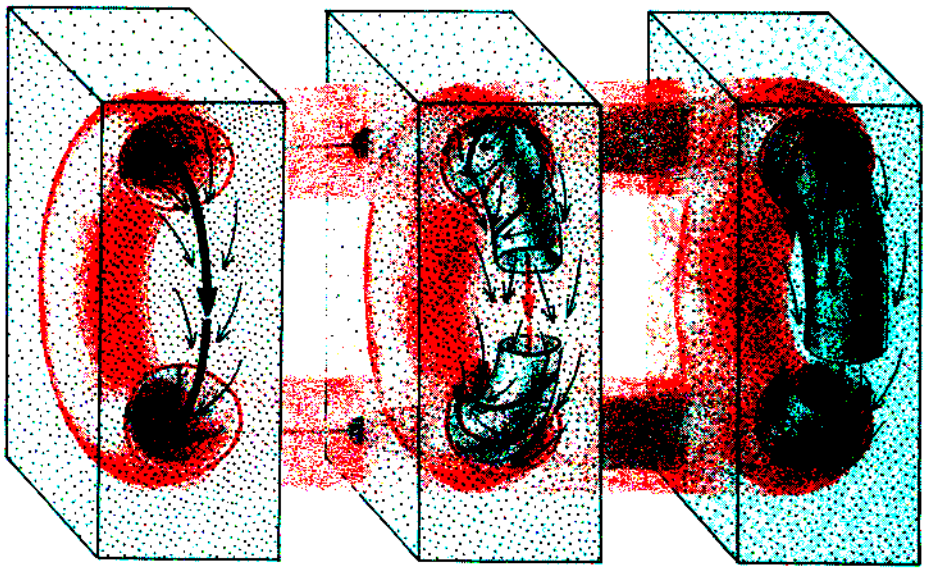

FIGURE 53. THE ONSET OF CHAOS. This phrase refers to a class of bifurcation events in which a simple (point or periodic) attractor turns into a chaotic attractor. Only a few of these have been studied, some by experimentalists, others by theoreticians. Here we show a typical example of the subclass known as *omega explosions*. The sequence begins with a fluctuating braid, as described in Figure 52. The onset of chaos involves changes in the underlying invariant torus (shaded black) of the braid. As the control is moved to the right, this torus develops a wave, which progresses into a fold and then a crease. As the pleated fold of the torus is pressed back down onto the torus by its attraction within the dynamic, the torus suddenly thickens, becoming a Cantor manifold (dimension 2+), which is the new attractor. Before the event there is a braid of periodic attractors. Afterward these are lost amid a thick toral attractor of the chaotic type. This example was discovered by R. Shaw in a study of forced oscillation on an analog computer.

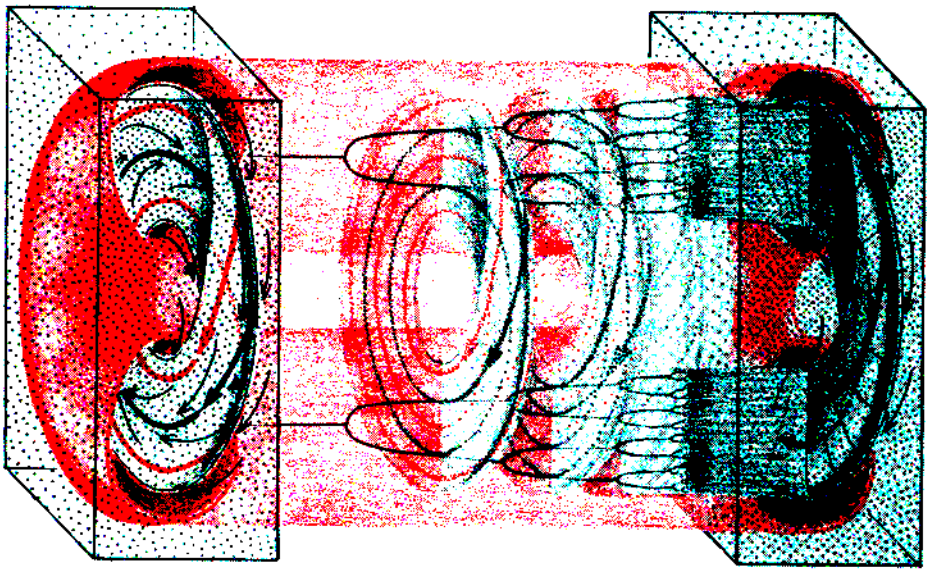

FIGURE 54. THE OCTAVE CASCADE. In another closely related context, an infinite sequence of octave jumps (see Figure 51) has been proven to be generic and to converge to an onset of chaos (Feigenbaum, 1978). After this limit point in the bifurcation set in control space, another bifurcation sequence converges from the right (Lorenz, 1980). This is a similar cascade of octave jumps, but all the attractors involved are chaotic. There is experimental evidence for the existence of this phenomenon in the omega explosion as well (Shaw, 1981), but it has not been proven to be actually an infinite sequence. Here we show the cascade of octave jumps for a periodic attractor traced on a substrate shaped like the Rössler attractor (see Figure 14), as suggested by the experimental work. The limit of the sequence is an onset of chaos bifurcation, in which the Rössler-looking substrate emerges as the attractor.

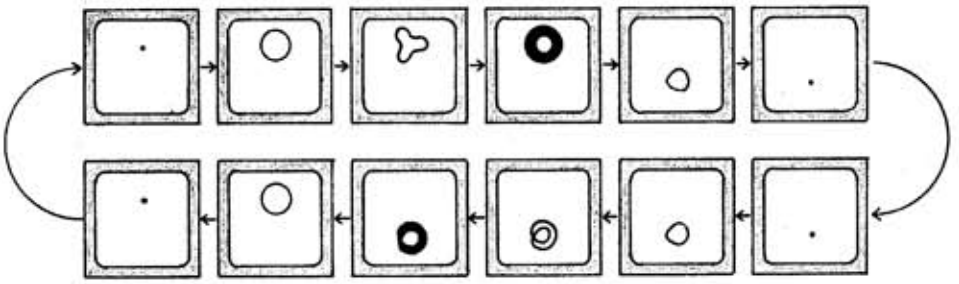

FIGURE 55. TYPICAL BIFURCATION SEQUENCES. In many experimental situations described by dynamical models with one control, moving the control in one direction results in a sequence of the bifurcations described singly in the preceding illustrations. Moving the control back again to the original value results in a similar, but different sequence. Here we illustrate some commonly observed sequences. Above, presented as the control moves to the right, a point attractor becomes periodic by excitation, then braided and chaotic—this is the *Ruelle–Takens sequence* (Ruelle and Takens, 1971). The chaotic attractor then disappears (by collision with its separatrix—a bifurcation anticipated by theory but not yet studied, or illustrated here). Below, a similar sequence is seen as the control is returned to the left, but different attractors are involved. Hysteresis may be observed. The dynamical model behind this phenomenon is shown in Figure 56.

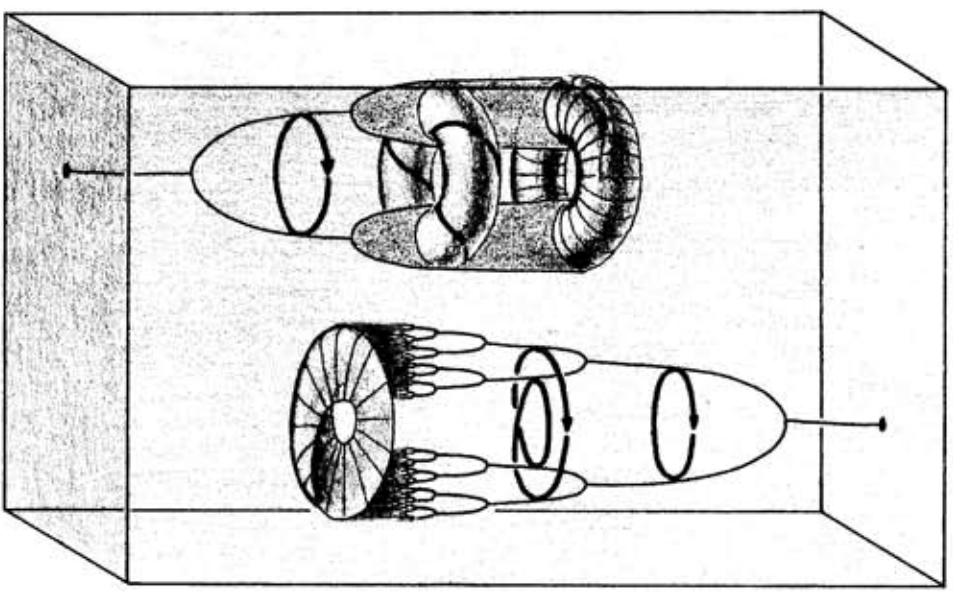

FIGURE 56. CHAOTIC HYSTERESIS. The bifurcation diagrams shown above are all atomic events. In real systems, compound models are encountered in which several of the atomic events are connected in a single bifurcation diagram. In these maps it is easy to understand hysteresis—the sure sign of catastrophic (as opposed to subtle) bifurcations. Here we show a fictitious bifurcation diagram in which two attractors undergo bifurcation separately, each in its own basin (except at the ends, where one or the other basin has disappeared). The observed behavior of the system is described in the preceding figure.

An Exemplary Application: Fluid Dynamics

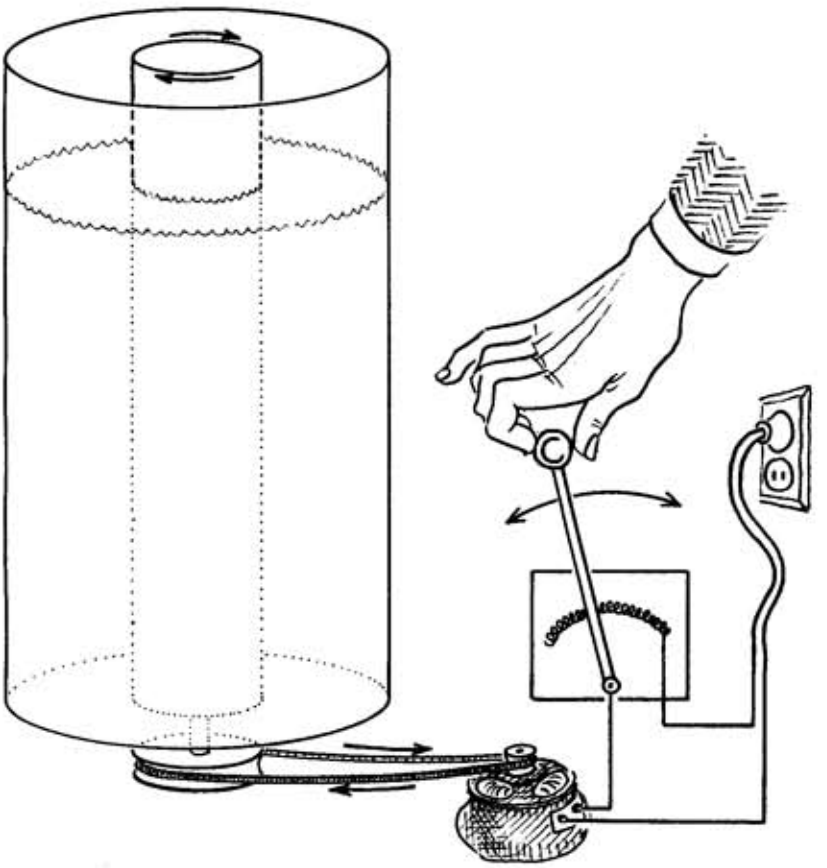

FIGURE 57. A STIRRING MACHINE. One way (not necessarily the best) to stir a cup of fluid is to rotate a swizzle stick in it. Great progress has been made in the study of turbulent fluid dynamics using this image. Since its earliest description a century ago, this experiment of Mallock and Couette has been repeated over and over, with ever-improved rods and cups. The onset of turbulence is carefully reproduced and observed with this apparatus. As the speed of stirring is increased beyond a critical (bifurcation) value, the expected flow of the fluid (in concentric, cylindrical lamellae) is replaced by *annular vortices*, patterns discovered by Taylor in 1923. Additional increase in the rate of stirring produces more bifurcations and, finally, turbulence.

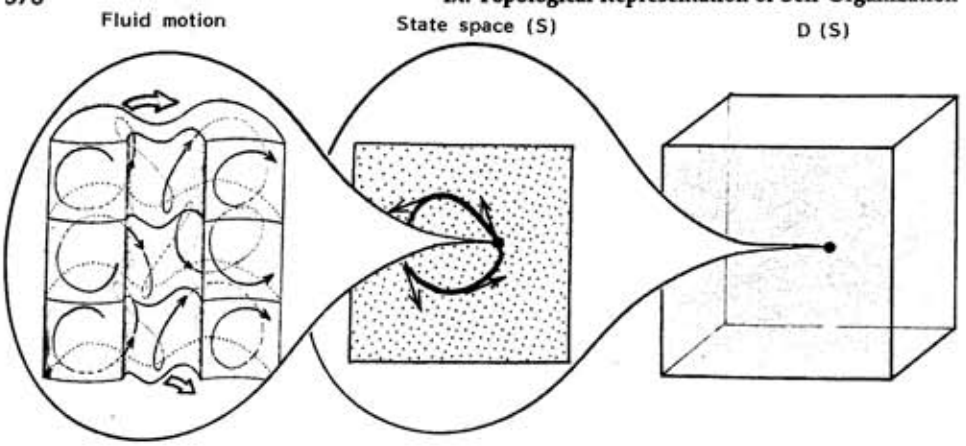

FIGURE 58. THE DYNAMICAL MODEL FOR TURBULENCE. To model this experimental situation with a dynamical system, the first step is the definition of the state space. One way to do this (due to Lagrange) is to record the fluid velocity vector at each point within the cup. This velocity vectorfield is considered to be the (instantaneous) state of the fluid motion and corresponds to a single point in the state space, S. This space, unfortunately, is infinite-dimensional. The change in the state of fluid motion as time passes is modeled by the partial-differential equations of Navier–Stokes. These may be considered (roughly) as a dynamical system on the state space, S. Thus, the Navier–Stokes equations are considered to be a system of ordinary differential equations on an infinite-dimensional state space and, therefore, a single point in the big picture, $D(S)$, instead of a system of partial differential equations on a three-dimensional fluid domain.

The behaviors of the fluid which are actually observed—Taylor vortices, for example—are attractors of this dynamical system on S. Furthermore, the rotation of the stirring rod is part of the Navier–Stokes system (the "boundary conditions"); thus, changes in the speed of rotation, c, move the dynamic $f(c)$ around in the big picture, $D(S)$. There are many technical problems involved in this model, which is still an active research area. Nevertheless, this model, studied by Ehrenfest and extensively used by Ruelle, makes the results of Dynamical Bifurcation theory applicable to the Couette–Taylor experiments and to fluid dynamics in general. The chaotic attractor in this dynamical model (from Ruelle and Takens, 1971) corresponds to turbulence in the fluid.

FIGURE 59. LAMELLAR FLOW in concentric cylinders occurs at slow stirring rates. Here we begin a sequence illustrating the successive events observed as the speed of stirring is gradually increased from zero. Initially the fluid is still. This condition is illustrated by the column on the left. The photo at top left shows the cylinder of fluid at rest, seen from the front. The drawing at left center shows the state as a velocity vectorfield; all velocity vectors are zero. The drawing at lower left shows the dynamical model: a point attractor at the origin (all velocity vectors zero) of the state space, S.

Next, in the column on the right, the stirring rate has increased slightly, and the flow is slow and lamellar. The photo of the fluid (top right) seen from the front is unchanged. But the velocity vectorfield (right center) is a pattern of horizontal, concentric circles, slowly rotating clockwise (as seen from above). The dynamical model (lower right) is again a point attractor in the infinite-dimensional state space, S, but it is no longer at the origin. The attractive point has drifted from the origin to a nearby point, corresponding to the lamellar flow, as the control (stirring speed) has been changed. This drift is indicated by the curve between the two lower drawings. There has been no bifurcation yet. (We are grateful to Rob Shaw for providing these photos of his work with Russ Donnelly's Couette machine at the University of Oregon.)

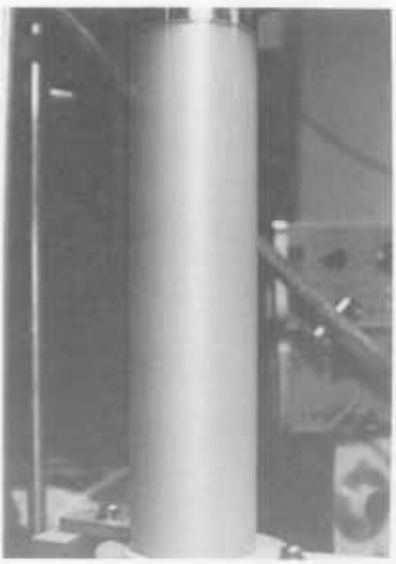

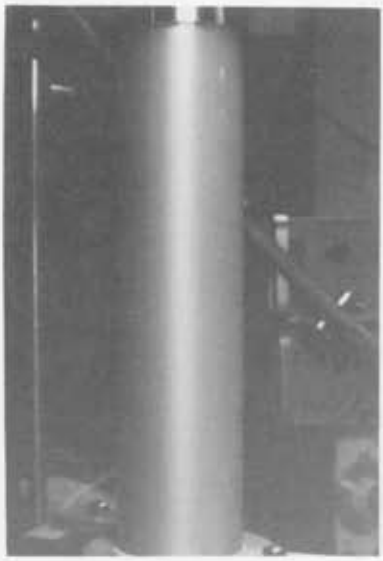

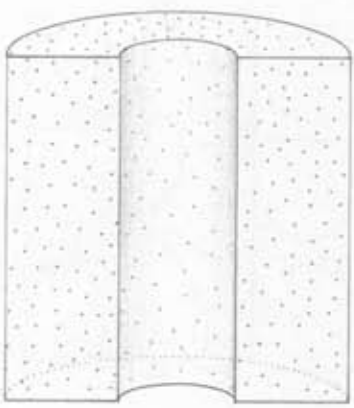

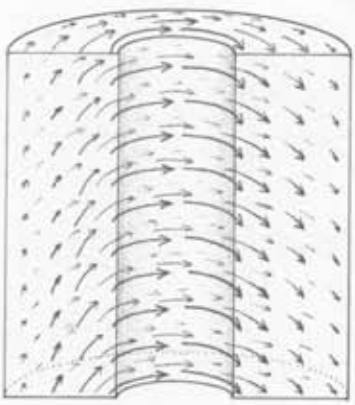

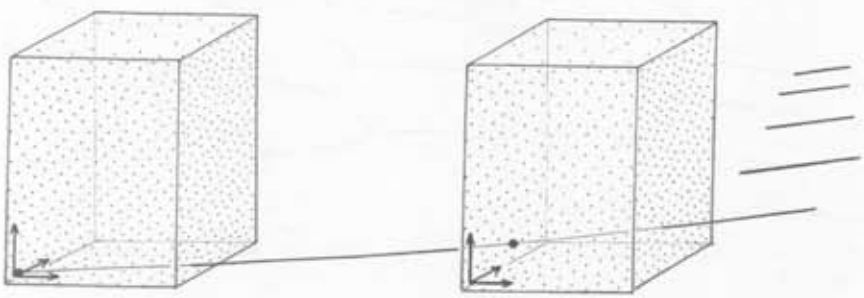

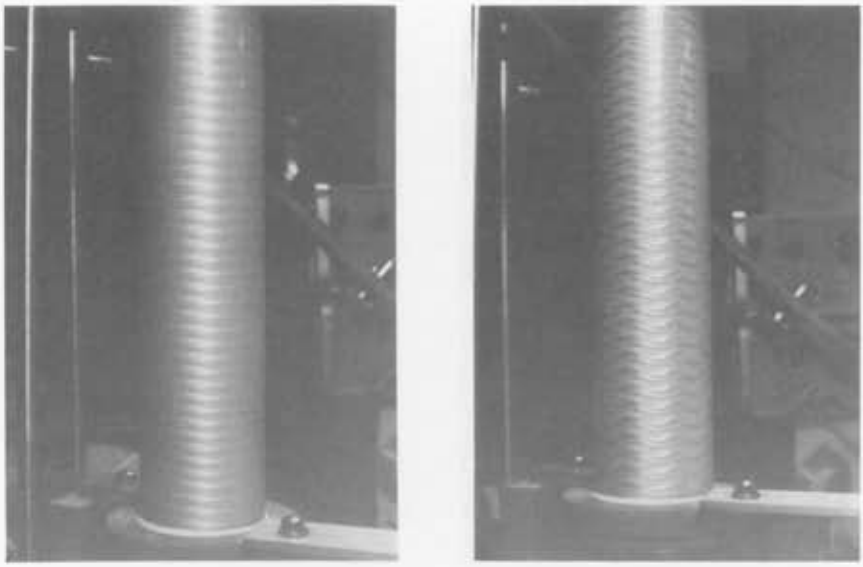

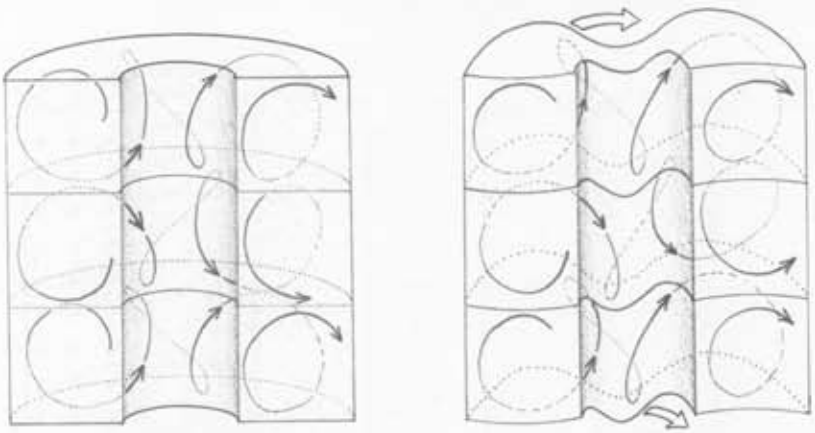

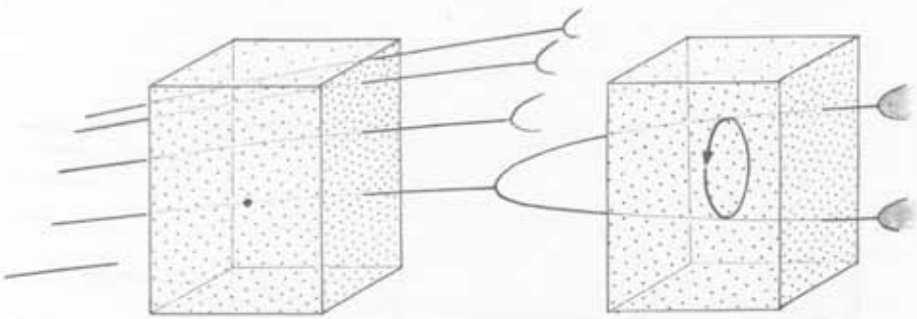

FIGURE 60. TAYLOR CELLS appear after additional increase in the rate of stirring. The column on the left illustrates the state of the fluid after the appearance of the annular vortices: photo of the fluid from the front; velocity vectorfield; and dynamical model (from top to bottom.) Even now the state of the fluid is still a rest point, because the velocity vectorfield is constant with respect to time, although it varies from point to point. It is possible that there has been no bifurcation yet in the dynamical model, because the attractor is still a point. Experimentalists, however, report that hysteresis is observed in the formation of the cells; the critical value of the speed of stirring for formation of the Taylor cells is higher than the critical value for their disappearance. Because hysteresis is the certain sign of catastrophic bifurcation, we suppose a kink (a static annihilation linked to a static creation bifurcation) in the track of the point attractor, from the lower right drawing of the preceding state (Figure 59) to the lower left here. Thus, we are creating a bifurcation portrait from the lower drawings of each column.

The bifurcation indicated by the kink between the preceding figure and this one is an outstanding example of the emergence of form through the *breaking of symmetry*. The lamellar flow has the symmetry of the vertical axis of the stirring rod, a one-dimensional symmetry. The stack of Taylor vortices has the symmetry of a discrete set of points within that axis, a zero-dimensional symmetry. One dimension of symmetry is lost when the attractor leaps from the lower branch of the kink to the upper branch.

The column on the right shows a new phenomenon, wavy vortices. Following increase in the stirring rate, the Taylor cells show waves which seem to rotate within the fluid (in the photo at top right). The velocity vectorfield (right center) now shows a periodic variation at each point within the fluid. The dynamical model (lower right) is, therefore, a periodic attractor. Between the two columns a Hopf bifurcation (Figure 50) has subtly taken place.

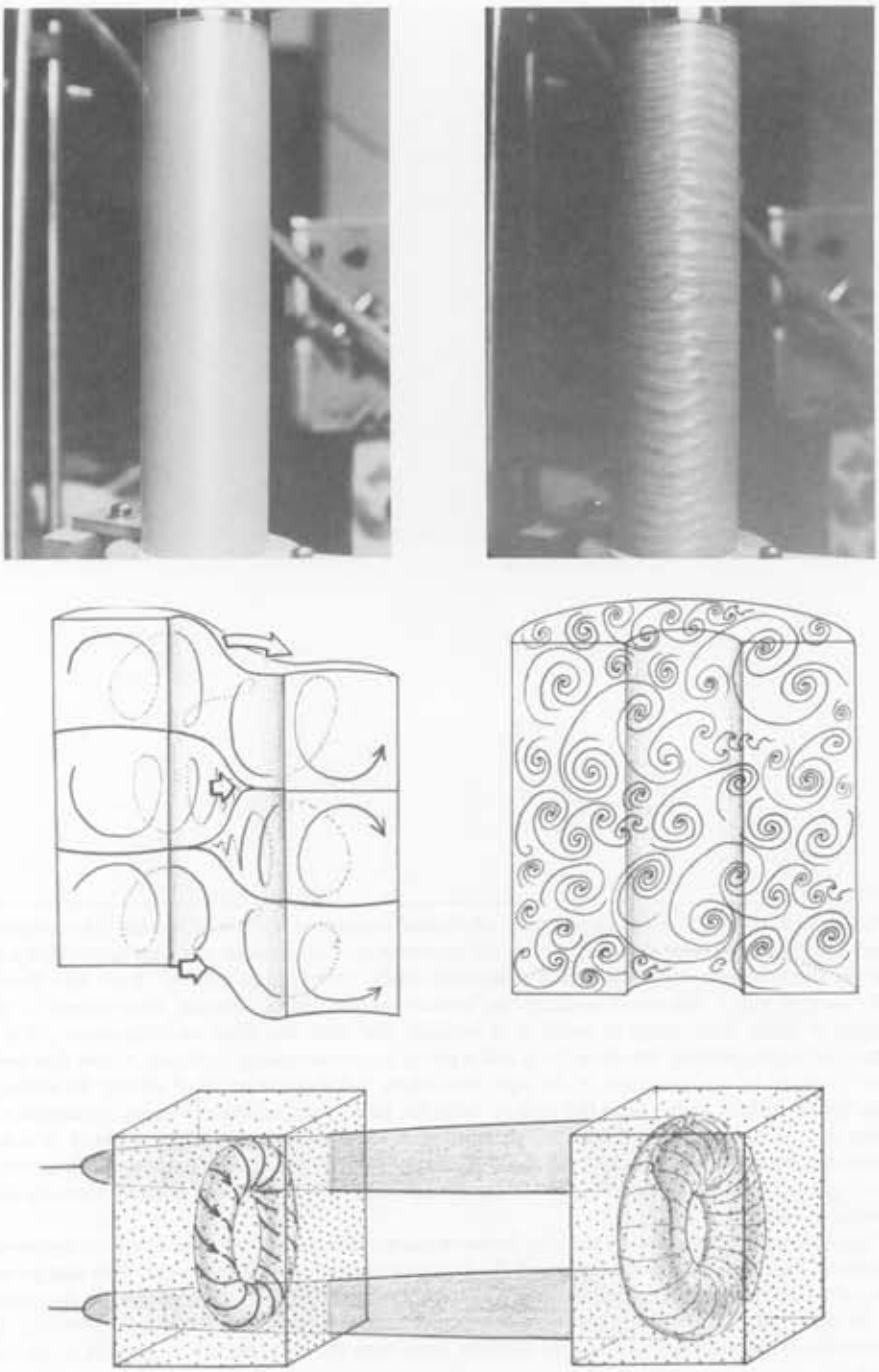

FIGURE 61. THE ONSET OF CHAOS follows additional increase of the speed of rotation of the central cylinder. After the Hopf bifurcation to wavy vortices, another bifurcation (observed by R. Shaw) produces pairs of dislocations of the annular cells. On the left this effect is shown as a braid bifurcation, which is pure speculation on our part, although experiments indicate the excitation of a new oscillatory mode. On the right, weakly turbulent fluid motion is shown where short bits of dislocated cells move chaotically about.

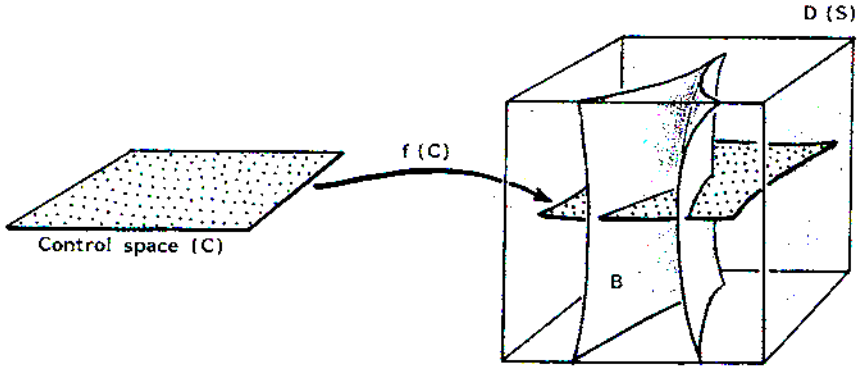

FIGURE 62. A DYNAMICAL SYSTEM WITH TWO CONTROLS. The knowledge we have gained of "generic arcs" in the big picture is small, but in some applications can be very powerful. Most applications, however, have more than one control, and our understanding of "generic disks" in the big picture—dynamical systems having multiple controls—has hardly begun. Here is an illustration of a generic two-dimensional disk in the big picture, corresponding to the *cusp catastrophe* of Elementary Catastrophe theory.

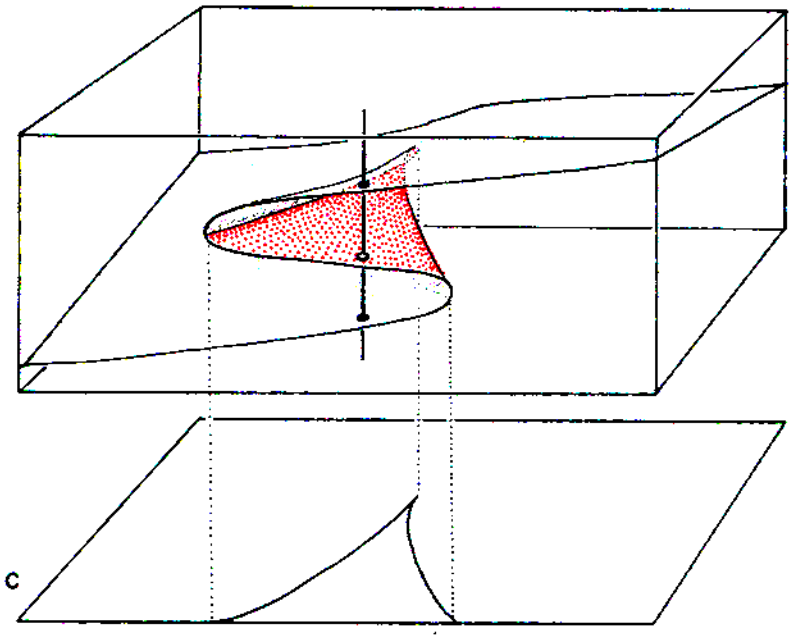

FIGURE 63. BIFURCATION DIAGRAM OF THE STATIC CUSP CATASTROPHE. In this example the state space is one-dimensional (vertical), and the control plane has two dimensions (horizontal); thus, the bifurcation diagram is actually three-dimensional, as shown here. The bifurcation set, B^I in C, is a cusp. For control values within this cusp, the one-dimensional AB portrait has two point attractors (black), separated by a point repellor (red). For control values outside the cusped bifurcation set there is only one attractor. There is another version of this event, the *periodic cusp catastrophe*, in which a periodic attractor bifurcates into two periodic attractors and a saddle cycle (see Figure 7). The two basins are separated by the periodic inset of this saddle cycle (see Figure 13). This periodic bifurcation has been found by Zeeman (1977) in a study of the forced Duffing equation.

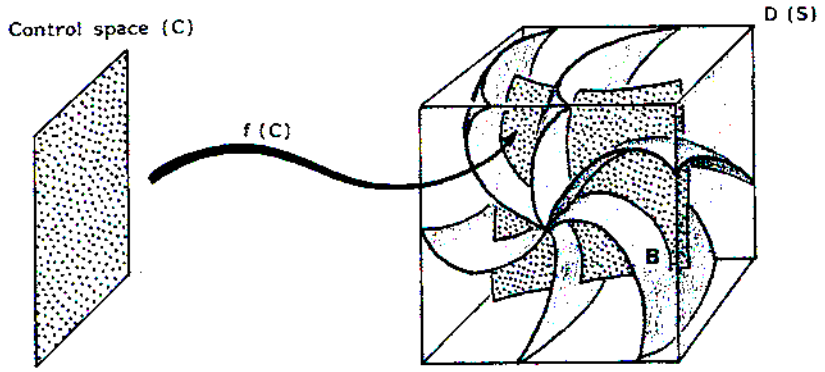

FIGURE 64. STARS IN THE BIG PICTURE also have been discovered. Here is a generic two-dimensional disk, stably intersecting a star of hypersurfaces of codimension one. This portrait corresponds to one of the few studied to date, the Andronov–Takens (2,−) bifurcation. It requires a state space of dimension two or more (Takens, 1973).

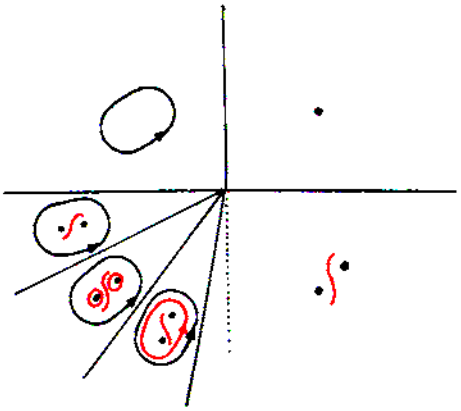

FIGURE 65. THE ANDRONOV–TAKENS BIFURCATION TABLEAU. With two controls and two state variables, the bifurcation diagram must be four-dimensional. Because direct visualization of this diagram is not possible, a simplified scheme has evolved, called the *method of tableaux*. Here we show the tableau for the Andronov–Takens bifurcation. The bifurcation set, B^f in C, consists of six rays radiating from a point. A generic arc bifurcation takes place across each ray. In each wedge the AB portrait is drawn, as if it lived in the control plane (which it does not). If one could steer the two control knobs very well, one could force the control point to pass through the vertex of the bifurcation set. For example, the point attractor (top) could be exploded into a periodic attractor and two attractive points (bottom). This event would never occur in a generic arc bifurcation or in an empirical device.

Complex Systems

Dynamics and studies of self-organization are two fields lying between mathematics and the sciences. They have been growing simultaneously, interacting and enriching each other. The concept of morphogenetic field and the big picture of Thom are products of this interaction, but the models provided so far by dynamics may be too simple to support the ideas now emerging in self-organization theory. We now propose some extensions of the concepts of dynamics that may prove useful in modeling hierarchical and complex systems.

Self-Regulation and Guidance Systems

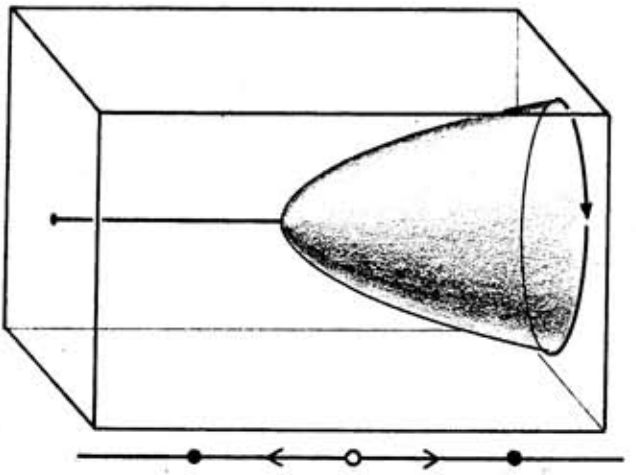

FIGURE 66. SELF-REGULATION OF ONE CONTROL. Given that we have a dynamical system depending on a control parameter, who turns the control knob? If it turns itself, through action of a dynamical subsystem on the control space itself, the model is called a self-regulating system. Here a typical dynamical system with one control, producing a Hopf bifurcation, is shown with a generic self-regulation vectorfield on the one-dimensional control space. Because this AB portrait on the line has only two point attractors, their basins separated by a point repellor, the control knob will seek one of these two attractive settings.

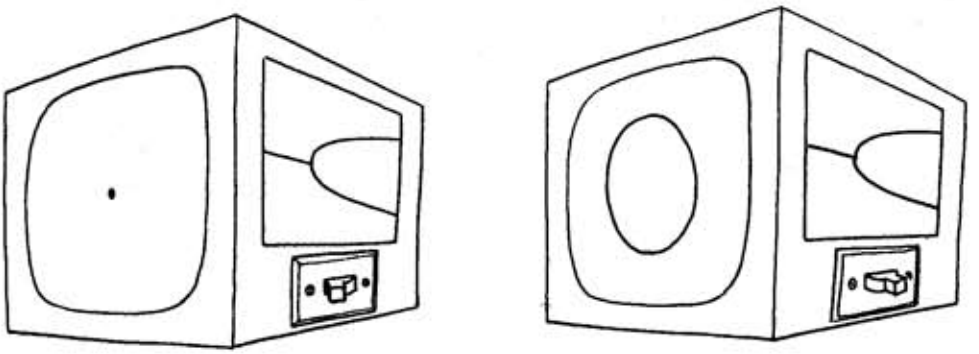

FIGURE 67. A MACHINE REPRESENTATION of the self-regulation system described above is this "electric stopwatch."

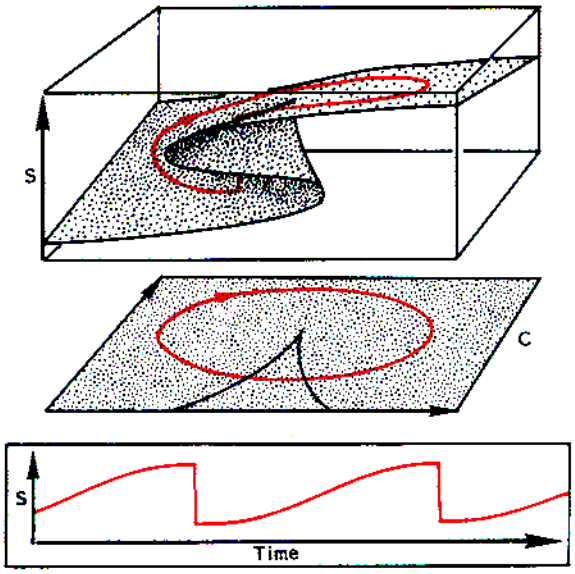

FIGURE 68. SELF-REGULATION OF TWO CONTROLS. Here a simple dynamical system with two-dimensional control space, the cusp of Figures 62 and 63, is endowed with a self-regulation vectorfield. This particular system has a single periodic attractor in the control space, C, with a virtual separatrix (a point repellor) within it. We always assume in these contexts that *the separatrices of the self-regulation dynamic are in "general position" with respect to the bifurcation set of the controlled dynamic*, in the sense that their intersection is as small as possible. The behavior of this system, introduced by Zeeman (1977) in a study of the electrical activity of neurons, is shown in the sawtooth-like time series recording the motion in the one-dimensional state space, S.

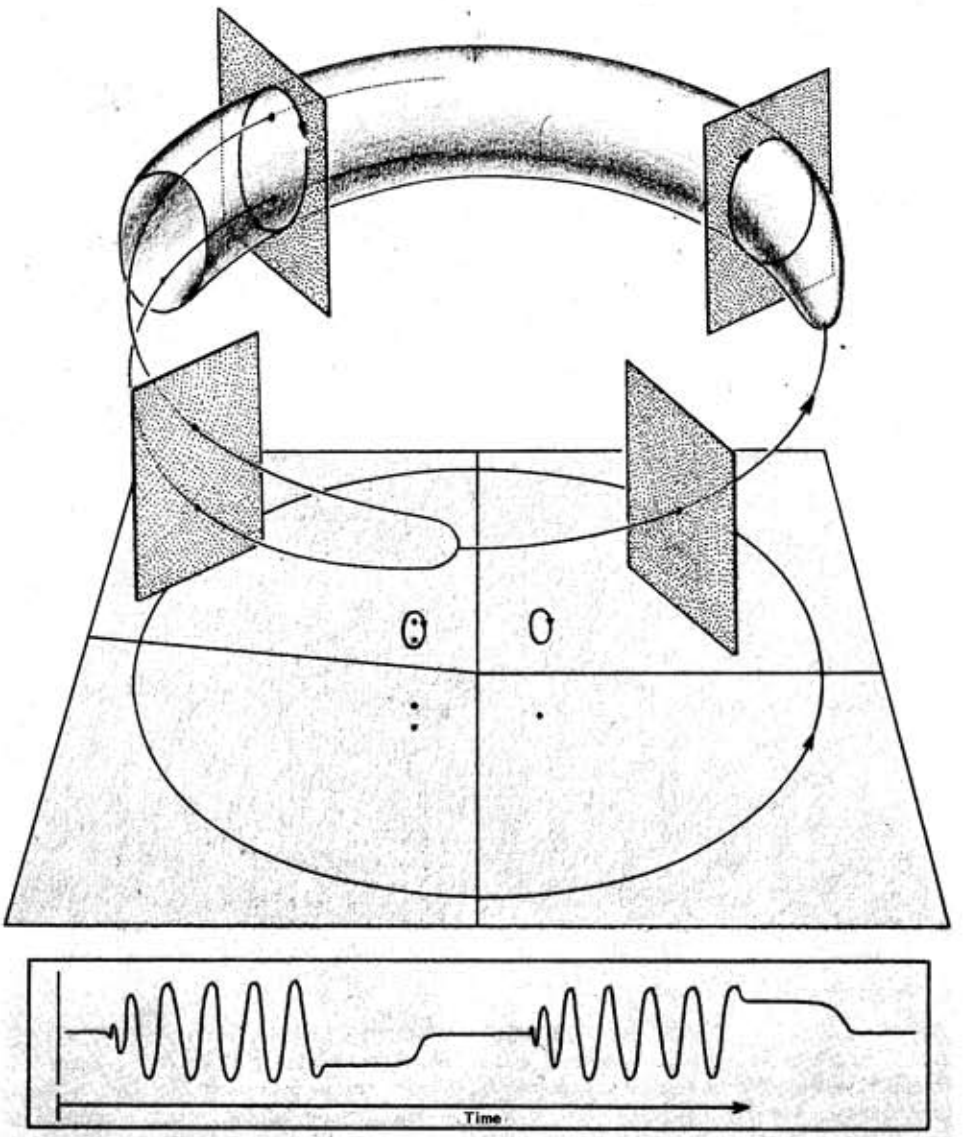

FIGURE 69. SELF-REGULATION WITH PERIODIC BEHAVIOR. The preceding example had a periodic attractor for its controls, but only a point attractor for its state dynamic. We show here a richer example, with the same control space and self-regulation dynamic, but with a state space of two dimensions. The bifurcation diagram is that of Andronov and Takens, shown in tableau form in Figures 64 and 65. Here we show the actual bifurcation diagram, obtained when the controls are restricted to the values along the periodic attractor on the control space. The time series corresponding to one of the two state variables also is shown. It resembles that of a stringed instrument rhythmically plucked. The direction in which it is plucked varies from cycle to cycle.

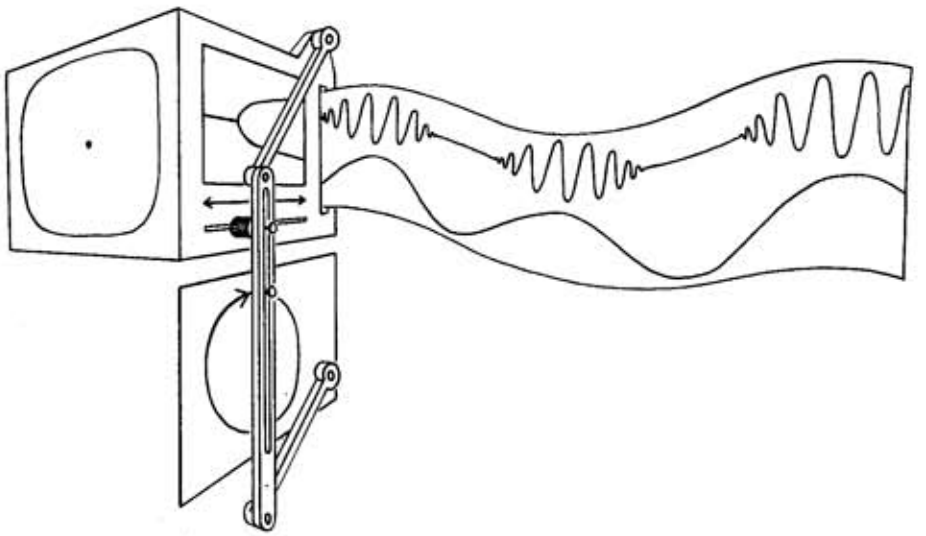

FIGURE 70. GUIDANCE SYSTEMS FOR ONE CONTROL. The self-regulation system is too limited for many applications, as this example shows. In this figure a dynamical system with one knob is controlled by a regulating vectorfield on an auxiliary space of two dimensions. A smoothly periodic variation of the control knob therefore is possible. In this example the controlled dynamic is again a Hopf bifurcation diagram, and the output time series of one of the two state variables is an intermittent oscillation. A similar system, described by Crutchfield, emits intermittent noise.

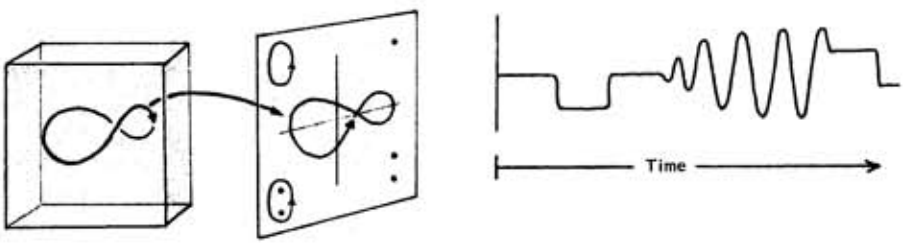

FIGURE 71. GUIDANCE SYSTEMS FOR MORE CONTROLS. By guidance system we mean a regulation vectorfield on an auxiliary space, B, and a *linkage map* from B to C, the control space of a dynamical system with controls, on a state space, S. Here is an example in which B, C, and S all have dimension two. The regulation dynamic on B has a periodic attractor, but the projection of this cycle from B into C by the linkage map is a loop that crosses itself. We shall call the projection of an attractor, in general, a *macron*. The controlled dynamic illustrated here is again the Andronov–Takens system of Figures 64, 65, and 69; the output is the time series shown. This is a periodic sequence of square waves and intermittent oscillation. Many other possibilities can be constructed with a guidance system as simple as this one.

Serial Coupling and Hierarchies

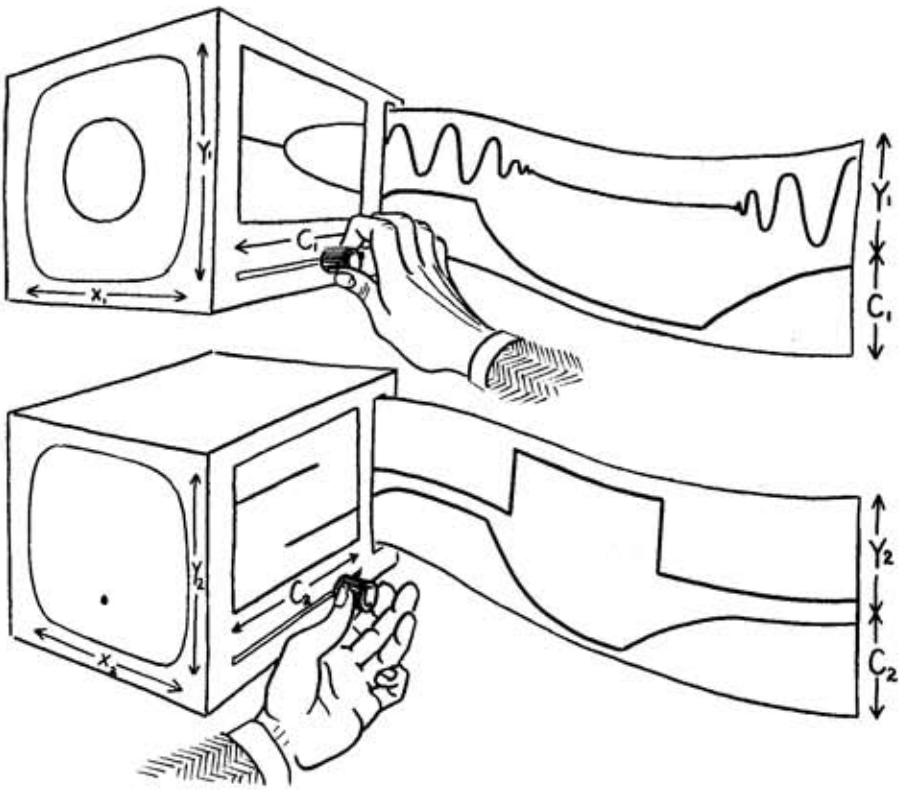

FIGURE 72. GUIDANCE WITH CONTROLS. In our sequence of portraits of gradually increasing complexity, we now consider two dynamical systems with controls. For example, let one be a subtle Hopf bifurcation (Figures 48–50) and the other a catastrophic kink exhibiting hysteresis (Figure 46, 47).

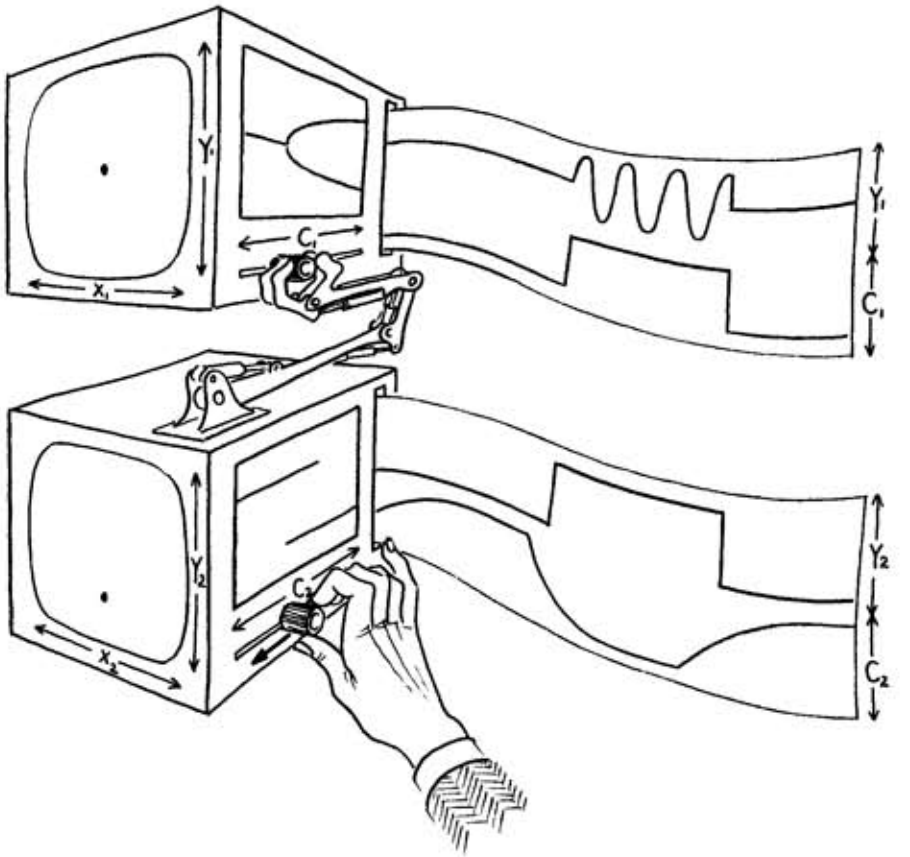

FIGURE 73. SERIAL COUPLING of these two systems means that a linking map is given from the state space of one, S^1, to the control space of the other, C^2. Thus, for a fixed value of the first control knob, the fixed dynamic on S^1 is a guidance system for the second system. But moving the first control knob changes the guidance dynamic. In the example illustrated here, moving the lower control knob full right, then full left, produces the time series shown for the guided system above. The lower control turns the oscillation abruptly on and off, with hysteresis.

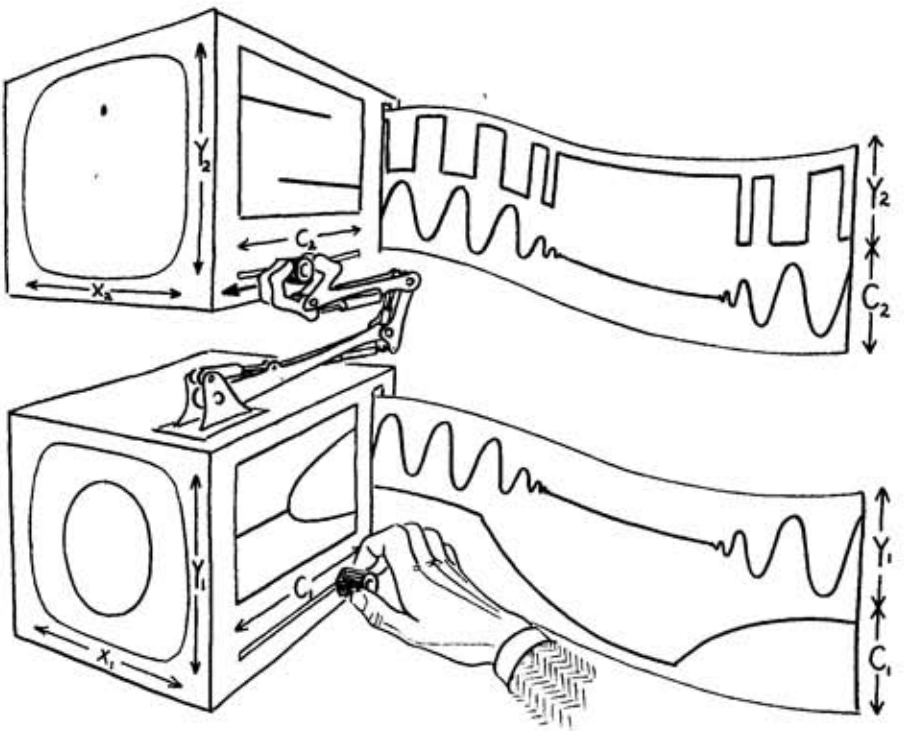

FIGURE 74. ANOTHER EXAMPLE is obtained by interchanging the roles of the two systems previously illustrated. Here the Hopf bifurcation controls the hysterical kink system. The lower control turns the square wave oscillator abruptly on and off, without hysteresis. (This type of system could be used, for example, to model the cAMP pulse relay activity of cellular slime mold—see Chapter 10.)

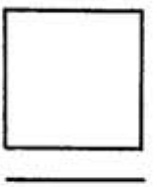

FIGURE 75. SYMBOLS for controlled dynamical systems may be made schematically by representing the control space as a horizontal line segment and the state space as a vertical line segment, regardless of the actual dimensions of these spaces. A single dynamical system with controls then is represented by a box with a line beneath it.

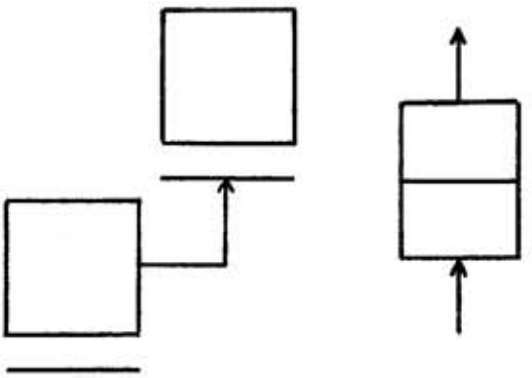

FIGURE 76. SERIAL COUPLING DIAGRAMS now may be constructed from these box symbols by connecting two of them by a directed line, representing a linking map from S^1 to C^2, as shown on the left. Alternatively, the simpler symbol on the right could be used.

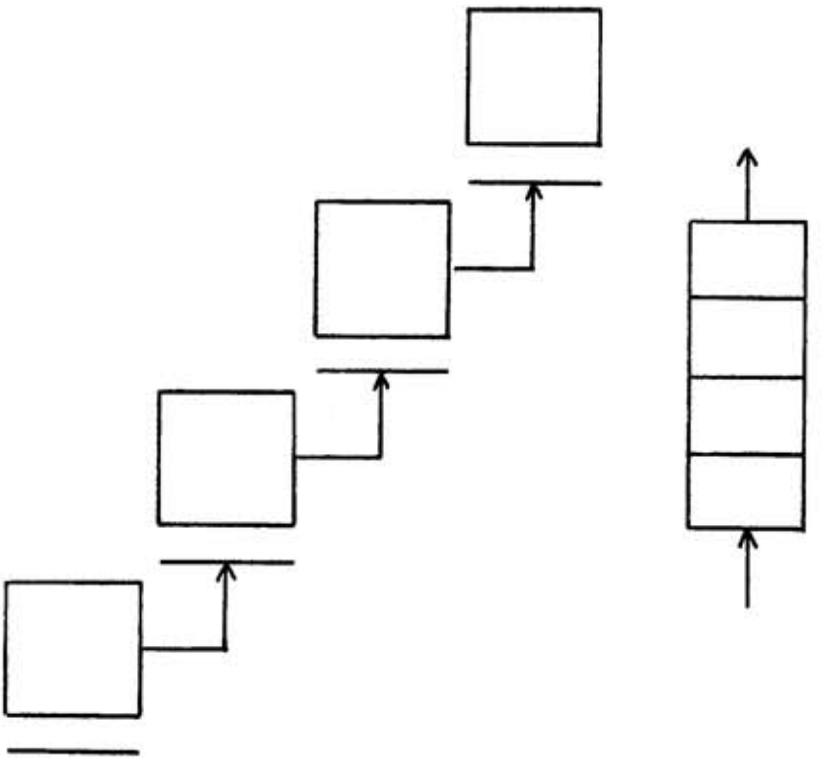

FIGURE 77. HIERARCHICAL SYSTEMS may be modeled by a sequence of serially coupled dynamical systems with controls, as shown here in two equivalent symbols.

Parallel Coupling, Complex Systems, and Networks

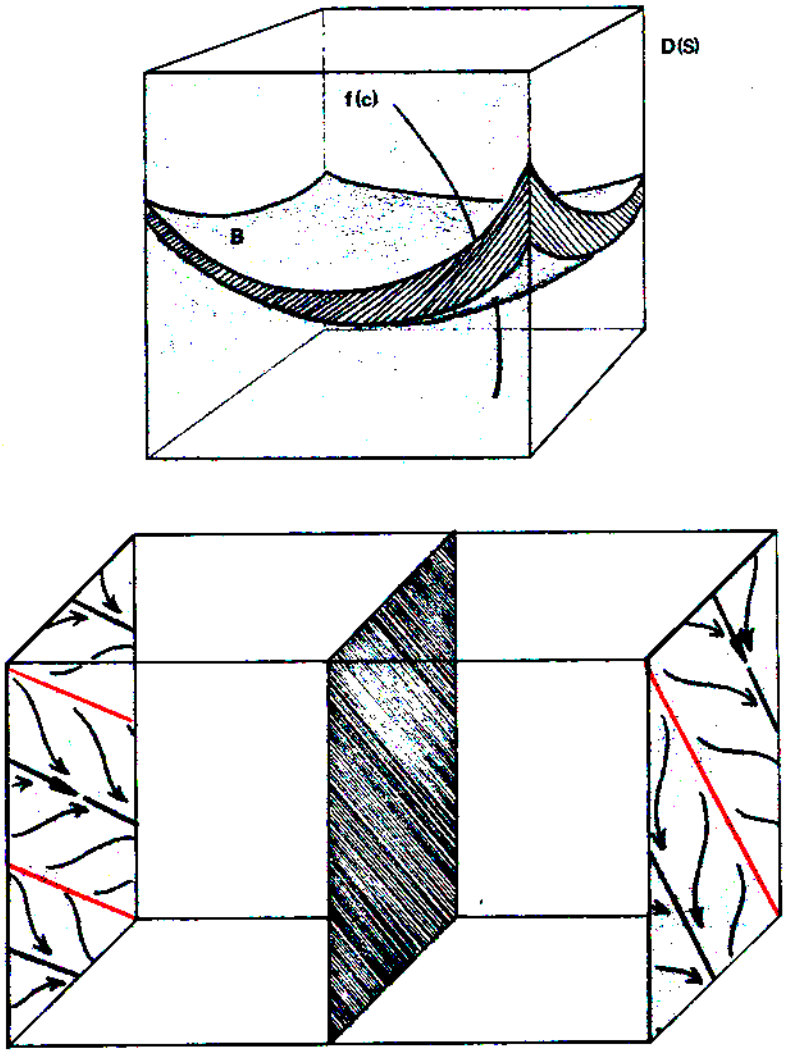

FIGURE 78. AN UNFOLDING of a bad (not structurally stable) dynamical system, X, in the bad set, B, denotes an embedding of X into a generic, controlled dynamical system, f, with control space, C; the result is that $f(C)$ in the big picture, $D(S)$, passes through B at X. This behavior requires that the dimension of C be not less than the codimension of B at X. The diagrams of catastrophic and subtle bifurcations (Figures 38–44 and 48–51) all represent unfoldings of a bad dynamical system. Figure 36 represents the fluctuating braid bifurcation, obtained by generically coupling two oscillators, as an unfolding of the bad dynamic for the uncoupled oscillators. We may consider the unfolding of the uncoupled oscillators as a sort of "dynamical multiplication" of them.

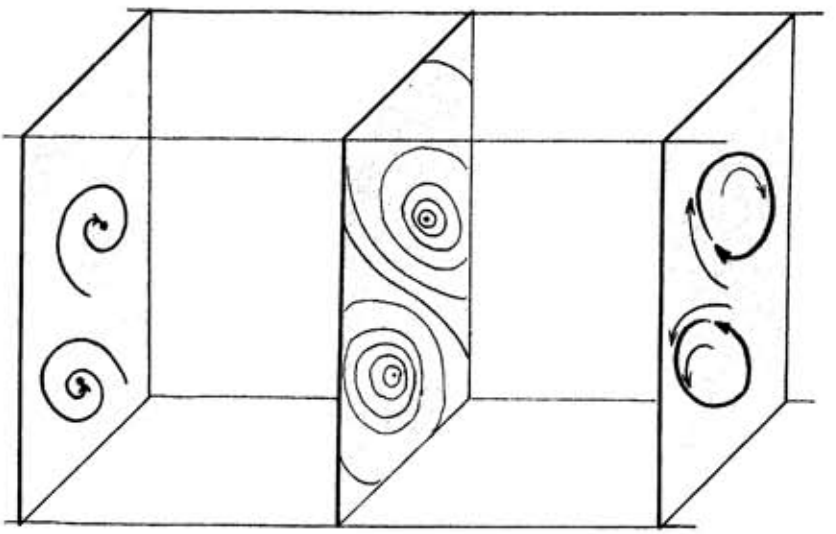

FIGURE 79. THE PARALLEL COUPLING OF DYNAMICAL SYSTEMS generalizes this dynamical multiplication to any dynamical system. Let X^1 be a dynamical system on a state space S^1, and let X^2 be another dynamic, on another state space, S^2. The product system, $X^1 \times X^2$, on the product space, $S^1 \times S^2$, probably will be bad. An unfolding of this product dynamic is called a parallel (or flexible) coupling of X^1 and X^2.

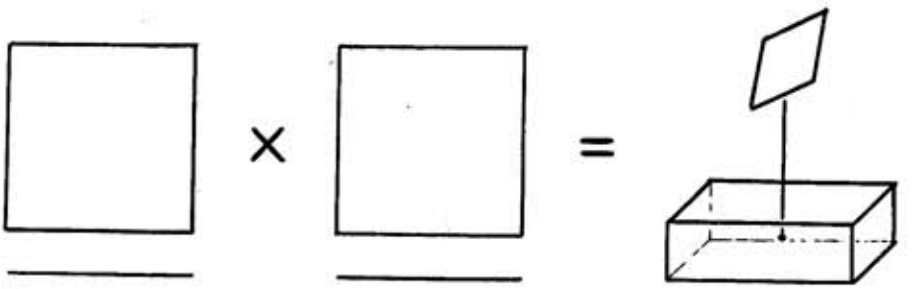

FIGURE 80. THE PARALLEL COUPLING OF CONTROLLED DYNAMICAL SYSTEMS adds a new control, C^0, for unfolding, to the controls C^1, and C^2, of the two controlled systems. The addition permits complete unfolding of the product of the interactions, as shown here.

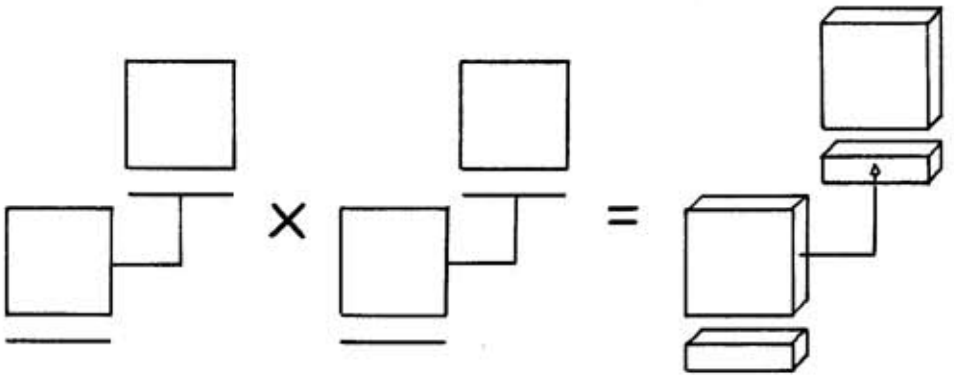

FIGURE 81. THE PARALLEL COUPLING OF GUIDANCE SYSTEMS repeats the coupling scheme for controlled systems, illustrated in the preceding figure, on both levels. To simplify the picture, we suppose that one new control, C^0, simultaneously unfolds both the guidance and the guided levels.

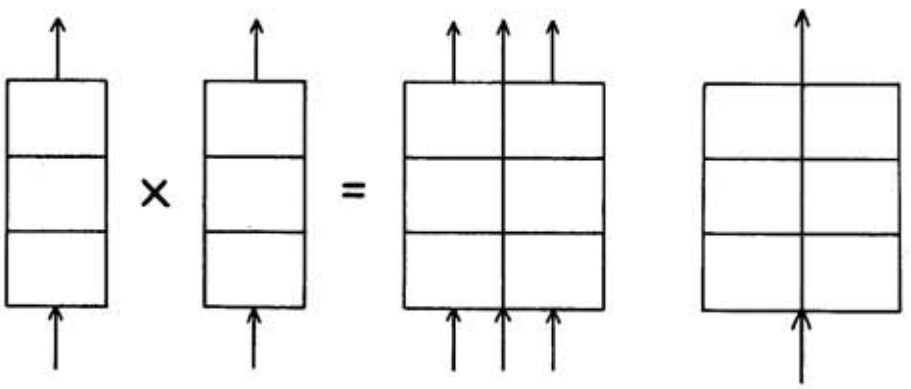

FIGURE 82. THE PARALLEL COUPLING OF HIERARCHICAL SYSTEMS (of the same number of levels) repeats the coupling scheme for guidance systems, illustrated in the preceding figure, on all levels of the hierarchy. (See Figure 75 for an explanation of the box symbol.) Again, one new set of controls, C^0, is assumed to control the flexible couplings on each level simultaneously and to unfold all of the couplings completely.

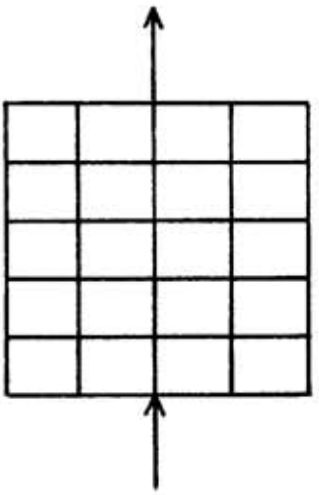

FIGURE 83. A COMPLEX SYSTEM may be made up of a set of hierarchical systems of the same length by assuming a parallel coupling between each pair of hierarchical systems in the set. The unfolding controls again are lumped into a single new control space, C^0. These controls are assumed to unfold all the parallel couplings at once.

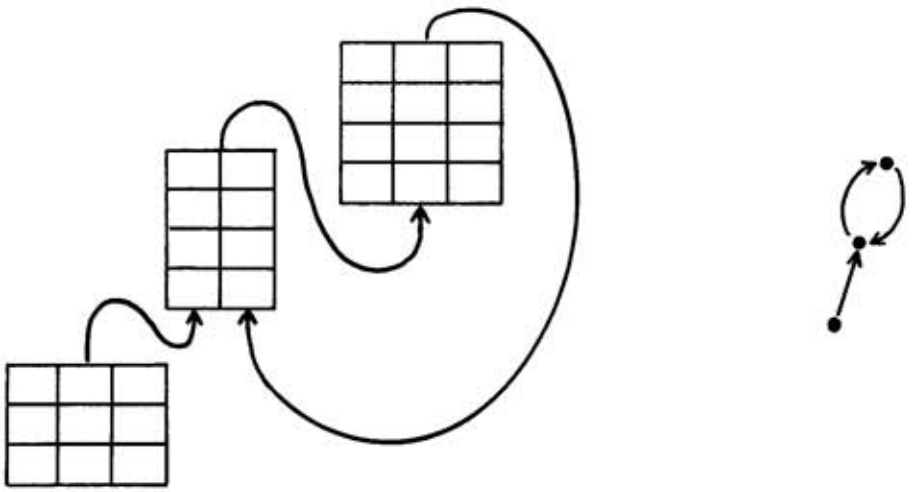

FIGURE 84. NETWORKS of complex systems are formed by directing the outputs of some to the controls of others. Here are two symbolic representations of a (simple) dynamical network. Chapter 30 relates the images and ideas of this chapter to the problem of self-organization.

ACKNOWLEDGMENTS. Some of the ideas presented here have been sharpened through discussion with colleagues. In particular, it is a pleasure to thank Alan Garfinkel for his emphasis on entrainment, Christopher Zeeman for his ideas on Cantor sets, and Rob Shaw for his description and photos of annular vortices in fluids.

References

Feigenbaum, M. (1978) Quantitative universality for a class of nonlinear transformations. *J. Stat. Phys.* **19**:25–52.

Herman, M. R. (1979) Sur la Conjugaison Differentiable des Diffeomorphismes du Cerole a des Rotations. *Publ. Math. IHES* **49**.

Lefshetz, S. (1950) *Contribution to the Theory of Nonlinear Oscillations.* Princeton University Press, Princeton, N.J.

Lorenz, E. (1963) Deterministic nonperiodic flow. *J. Atmos. Sci.* **20**:130–141.

Lorenz, E. (1980) Noisy periodicity and reverse bifurcation. *Ann. N.Y. Acad. Sci.* **357**:282–291.

Neimark, Y. I. (1959) On some cases of dependence of periodic motions on parameters. *Dokl. Akad. Nauk SSSR* **129**:736–739.

Peixoto, M. (1962) Structural stability on two-dimensional manifolds. *Topology* **2**:101–121.

Poincaré, H. (1885) Sur l'équilibre d'une masse fluide animée d'un mouvement de rotation. *Acta Math.* 7:259–380.

Pugh, C. C., and M. Shub (1980) Differentiability and continuity of invariant manifolds. Preprint, Queens College, Flushing, N.Y.

Rössler, O. E. (1979) Chaos. In: *Structural Stability in Physics*, W. Güttinger and E. Eikemeyer (eds.). Springer-Verlag, Berlin, pp. 290–309.

Ruelle, D., and F. Takens (1971) On the nature of turbulence. *Commun. Math. Phys.* **20**:167–192.

Shaw, R. (1981) Strange attractors, chaotic behavior, and information flow. *Z. Naturforsch.* 36a:80–112.

Sotomayor, J. (1974) Generic one-parameter families of vector fields in two-dimensional manifolds. *Publ. Math. I. H. E. S.* **43**:5–46.

Takens, F. (1973) Introduction to global analysis. *Commun. Math. Inst., Rijksuniversiteit Utrecht* **2**:1–111.

Thom, R. (1972) *Stabilité structurelle et morphogénèse: Essai d'une théorie générale des modeles.* Benjamin, New York.

Whitehead, A. N. (1925) *Science and the Modern World.* Macmillan Co., New York.

Zeeman, C. (1976) The classification of elementary catastrophes of codimension < 5. In: *Structural Stability, the Theory of Catastrophes, and Applications in the Sciences*, P. Hilton (ed.). Springer-Verlag, Berlin, pp. 263–327.

Zeeman, E. C. (1977) *Catastrophe Theory: Selected Papers.* Addison–Wesley, Reading, Mass.